WES-MP-

MISCELLANEOUS PAPER S-77-24

# SUBSURFACE EXPLORATION IN ALLUVIAL TERRAIN BY SURFACE GEOPHYSICAL METHODS.

by

William L. Murphy

Soils and Pavements Laboratory
U. S. Army Engineer Waterways Experiment Station
P. O. Box 631, Vicksburg, Miss. 39180

December 1977

Final Report.

85 p.

D D C
RECEIVED
JAN 31 1978
F

038 100

| REPORT DOCUMENTATION PAGE | | READ INSTRUCTIONS BEFORE COMPLETING FORM |
|---|---|---|
| 1. REPORT NUMBER <br> Miscellaneous Paper S-77-24 | 2. GOVT ACCESSION NO. | 3. RECIPIENT'S CATALOG NUMBER |
| 4. TITLE (and Subtitle) <br> SUBSURFACE EXPLORATION IN ALLUVIAL TERRAIN BY SURFACE GEOPHYSICAL METHODS | | 5. TYPE OF REPORT & PERIOD COVERED <br> Final Report |
| | | 6. PERFORMING ORG. REPORT NUMBER |
| 7. AUTHOR(s) <br> William L. Murphy | | 8. CONTRACT OR GRANT NUMBER(s) |
| 9. PERFORMING ORGANIZATION NAME AND ADDRESS <br> U. S. Army Engineer Waterways Experiment Station <br> Soils and Pavements Laboratory <br> P. O. Box 631, Vicksburg, Miss. 39180 | | 10. PROGRAM ELEMENT, PROJECT, TASK AREA & WORK UNIT NUMBERS |
| 11. CONTROLLING OFFICE NAME AND ADDRESS <br> U. S. Army Engineer Division, <br> Lower Mississippi Valley <br> P. O. Box 80, Vicksburg, Miss. 39180 | | 12. REPORT DATE <br> December 1977 |
| | | 13. NUMBER OF PAGES <br> 79 |
| 14. MONITORING AGENCY NAME & ADDRESS(if different from Controlling Office) | | 15. SECURITY CLASS. (of this report) <br> Unclassified |
| | | 15a. DECLASSIFICATION/DOWNGRADING SCHEDULE |

16. DISTRIBUTION STATEMENT (of this Report)

Approved for public release; distribution unlimited.

17. DISTRIBUTION STATEMENT (of the abstract entered in Block 20, if different from Report)

JAN 31 1978

F

18. SUPPLEMENTARY NOTES

19. KEY WORDS (Continue on reverse side if necessary and identify by block number)

Alluvium
Geophysical exploration
Resistivity surveys
Seismic refraction method
Subsurface exploration

20. ABSTRACT (Continue on reverse side if necessary and identify by block number)

Field tests were conducted at several sites in Louisiana to determine the effectiveness of two geophysical tools for detecting and locating subsurface geological features in alluvial terrain. The hammer seismic refraction technique, using a hammer source and portable seismograph, and the surface electrical resistivity method, using a D.C.-powered resistivity meter and current source, were investigated. Seismic refraction lines and resistivity soundings and profiles were run concurrently at each site. Boring control was used where available to aid in interpretation of the geophysical data. (Continued)
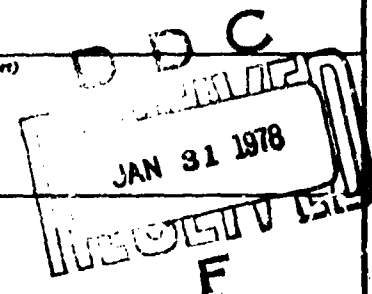
DD FORM 1473 EDITION OF 1 NOV 65 IS OBSOLETE

20. ABSTRACT (continued).

The resistivity profiling (fixed electrode spacing) technique was the most successful of the three methods, detecting or locating the targeted geologic feature at three of the four sites tested. The resistivity sounding (expanding electrode spacing) technique delineated shallow features but was ineffective at depth. The hammer seismic technique also achieved only limited success at depth, attributed primarily to attentuation of the seismic signals by loose near-surface materials. Surveys were precluded at one site by the presence of certain man-made features that interfered with the collection of usable data.
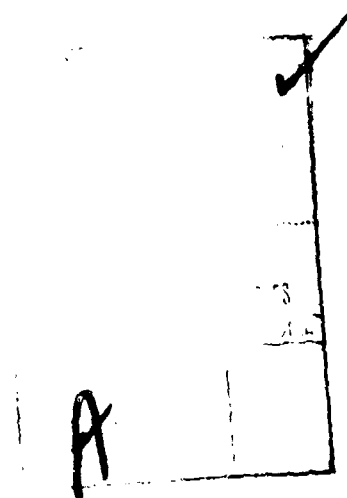
# PREFACE

This study was authorized in a first endorsement dated 12 September 1975 to a letter from the Director, U. S. Army Engineer Waterways Experiment Station (WES), to the Division Engineer, U. S. Army Engineer Division, Lower Mississippi Valley (LMVD), dated 12 April 1975.

The conduct of this study was accomplished by Messrs. W. L. Murphy of the Engineering Geology and Rock Mechanics Division (EGRMD), Soils and Pavements Laboratory, WES; Don Douglas of the Earthquake Engineering and Vibrations Division, Soils and Pavements Laboratory, WES; and Kenneth Holloway, Geology Section, Foundations and Materials Branch, LMNED-FE. The report was prepared by Mr. Murphy. Direct supervision of this study was provided by Mr. W. B. Steinriede, Chief, Geology Branch, EGRMD. General supervision was provided by Mr. Don C. Banks, Chief, EGRMD, and Mr. James P. Sale, Chief, Soils and Pavements Laboratory.

Director of WES during the conduct of this study was COL John L. Cannon, CE. Technical Director was Mr. F. R. Brown.

# CONTENTS

## CONVERSION FACTORS, U. S. CUSTOMARY TO METRIC (SI)
## UNITS OF MEASUREMENT

U. S. customary units of measurement used in this report can be converted to metric (SI) units as follows:

| Multiply | By | To Obtain |
|---|---|---|
| pounds (mass) | 0.4535924 | kilograms |
| feet | 0.3048 | metres |
| miles (U. S. statute) | 1.609344 | kilometres |
| feet per second | 0.3048 | metres per second |
| degrees (angular) | 0.01745329 | radians |

# SUBSURFACE EXPLORATION IN ALLUVIAL TERRAIN BY SURFACE GEOPHYSICAL METHODS

## PART I: INTRODUCTION

### Background

1. Restraints caused by urbanization and environmental concern have led to increasing emphasis on the use of remote sensing and low-energy surface and subsurface exploration systems in Corps foundation investigations and construction material surveys. The increasing cost of borings is often the basis for use of widely-spaced borings in pre-construction foundation investigations with subsequent loss of detail regarding subsurface conditions. The use of surface geophysical techniques to obtain subsurface data offers a means of economically supplementing limited borehole investigation and of aiding in more efficient placement of borings. Resistivity and seismic refraction methods are being used for various investigative purposes in upland areas and in areas containing hard rock materials. There is little reference in the literature, however, to applications in alluvial and deltaic areas. In these areas soils are variable both laterally and vertically, may contain appreciable amounts of organic matter, and often are characterized by shallow, even surface-exposed, groundwater conditions.

2. Urban areas also have features that affect the acquisition of subsurface data. Constraints on high-energy geophysical methods such as explosive seismic techniques are expected in cities, a problem that can be overcome by use of the hammer seismic device. Urban areas also contain anomalies in the form of rail lines, buried and overhead electrical cables, sewer lines, and fences that affect either seismic signals or electrical current patterns. The capability of seismic and resistivity surveys to operate effectively under these circumstances should be demonstrated.

3. The New Orleans District of the Lower Mississippi Valley Division (LMVD), U. S. Army Corps of Engineers, provides a variety of projects, such as levee and drainage structure locations and setbacks, lock investigations, location of construction materials, and routine maintenance of flood control and other structures in diverse hydrologic and geologic conditions in which surface geophysical methods can be investigated and procedures developed.

## Purpose and Scope

4. This study investigated the effectiveness of seismic refraction using a hammer source and surface electrical resistivity methods in determining the presence, depth, and characteristics of subsurface geologic features in an alluvial terrain. The study also investigated the ability of these techniques to function in an urban environment. The equipment used was limited to a single-channel, signal-enhancement refraction seismograph and a direct-current resistivity meter. The two systems were used to obtain complementary data at each of four sites. The geologic materials encountered were all unconsolidated, dry to saturated, and ranged from clays through sands and gravels.

5

PART II: SITES, EQUIPMENT, AND METHODS

## Description of Sites

5. Geophysical surveys were run at four sites in the New Orleans District and attempted at one other site. Figure 1 shows the general locations of the four sites. The first s e is on the left bank of the Old River outflow channel, west of the Old River Control Structure, in the Fort Adams and Turnbull Island 7-1/2 minute quadrangles. The target at this site was a buried clay plug filling a portion of an abandoned Mississippi River channel. The second site is near the proposed location for Lock and Dam No. 3 on the Red River in central Louisiana, located in the Boyce, Louisiana, quadrangle. Surveys there attempted to locate the contacts between the point bar-backswamp system of the Red River and the upland Pleistocene terrace deposits. An attempt was also made to determine the depth to the underlying Tertiary bedrock.

6. The third site is in north-central New Orleans along the west levee of the Metairie Outfall Canal. The site is located in the Spanish Fort and New Orleans East quadrangles. An ancient buried beach has been mapped previously in this vicinity and the geophysical investigation was directed toward finding the southern edge of the beach and determining the depth to its top. An alternate site on the Inner Harbor Navigation Canal, New Orleans, containing the buried beach was also visited, but the existence of certain man-made structures at the site made it impossible to collect usable data, as discussed in Part III of this report. The fourth site, located in the New Orleans West quadrangle, is along a recently cleared railroad right-of-way on Nine Mile Point, south of the Mississippi River. The geologic section consists of point bar to the north, contacting backswamp materials to the south, overlain partially by natural levee deposits. The object of the surveys there was to locate the contact between point bar and backswamp materials, determine the thickness of natural levee deposits, and, if possible, detect the

6

contact with the underlying Pleistocene deposits at depth. Detailed locations and descriptions of these sites are given in Part III.

## Equipment

7. The seismic refraction surveys were run with a Bison Model 1575B single-channel signal-enhancement seismograph with strip-chart recorder (Figure 2). The system uses a single geophone to receive seismic signals generated by striking a metal plate on the ground with a sledge hammer. A 16-lb* hammer and a steel striking plate were used for all the seismic surveys in this study. Signal arrival times are read to the nearest tenth of a millisecond. The geophone amplifier gain can select from 0 to 99 decibels (db) in 1 db increments. A Keck Model IC-69 direct-current resistivity meter was used in the electrical surveys (Figure 3). The resistivity meter draws up to 400 microamperes while operating and gives a reading in ohms to the nearest thousandth ohm. Power for the resistivity determination is supplied by four 45-volt dry cell batteries connected in series by a switch to allow use of one or more batteries at a time. Current electrodes are copper-clad steel stakes. Porous ceramic pots filled with copper sulphate are used as potential electrodes.

## Seismic Interpretation Methods

8. The seismic surveys were interpreted using standard seismic (compressional wave) velocity and time intercept/critical distance equations. Signal arrival times were determined on the seismograph oscilloscope and plotted on linear graph paper for each hammer impact station. The resulting time-distance curves yielded depths to interfaces between layers of different seismic velocity, seismic velocities of the various layers, and dip of the contacts. Reversed profiles were

---

* A table of factors for converting U. S. customary units of measurement to metric (SI) units is presented on page 3.

run when necessary to detect dipping contacts. The reader is referred to the many texts on the refraction seismic technique for explanation of t e theory and derivation of the equations (see, for example, Dobrin,[1] Chapter 5; Redpath[2]; Musgrave,[3] Section 5; Zohdy,[4] pages 67-84; and Mooney[5]).

## Resistivity Interpretation Methods

9. Two kinds of resistivity surveys were run for this study. A resistivity sounding was run about a fixed central point to determine changes with depth, and a resistivity profile, in which the entire electrode array is moved along a line, was run to determine lateral changes. The Schlumberger array was selected for the sounding surveys because the array allows recognition of the presence of lateral inhomogeneities and because field procedures in sounding are faster with it than with the Wenner array. The Wenner array, on the other hand, is simpler to use in a profiling survey because its electrode spacings are equal. Field procedures for applying the various arrays are discussed below. Soundings were interpreted by the curve matching technique, in which field plots of apparent resistivity versus electrode spacing are matched against master curves. The field and master curves are matched directly when possible and otherwise by the use of auxiliary curves. The master curves are mathematically derived curves of apparent resistivity versus electrode spacing representing a variety of ideal subsurface conditions. The curves used in this study are those of Orellana and Mooney,[6] plotted on a modulus of 62.5 mm/cycle. Field curves were plotted on double logarithmic graph paper of identical scale obtained from Aerni-Leuch, Bern, Switzerland, Number 551. True resistivities and depths to layers of contrasting resistivities can be computed by the curve matching process (Orellana and Mooney,[6] Part III). The resistivity profile data were interpreted qualitatively by analysis of the shape of the field curve. Part III of this report demonstrates the interpretation procedures. The reader should see the following references for theoretical considerations and further field applications of

8

resistivity methods. Orellana and Mooney[6]; Keller and Frischknecht[7]; Dobrin,[8] Chapter 17; Zohdy,[4] pages 5-63; and Van Nostrand and Cook[9].

## Refraction Seismic Field Procedures

10. The seismograph and strip-chart recorder are set up in the back of a carryall or similar vehicle for protection from the weather. The geophone is implanted into firm ground in a level position at station zero near the seismograph. A cable connects the geophone with the seismograph. Ruled tapes for positioning the hammer stations are laid out in opposite directions from station zero. Another cable connects the hammer trigger switch to the seismograph. For the investigation, hammer stations were run usually at 5-ft spacings out to 100 ft, and then at 10- or 20-ft spacings out to the maximum distance at which usable signals were obtained. The short initial spacings allow better definition of shallow features such as soil interfaces, the weathered zone, and the groundwater interface. The steel striking plate was placed successively at each impact station and struck repeatedly with the hammer until a sufficiently enhanced signal was obtained on the seismograph oscilloscope. Figure 4 illustrates the basic features of a refraction seismic line.

11. The seismograph used in this investigation displays travel time in milliseconds on an oscillograph as a pointer is moved to the proper point on the signal trace. The travel time is plotted against the appropriate hammer station on the travel time-distance graph. The procedure was repeated for hammer stations in the opposite direction from station zero, and those data were plotted as a separate curve. If the curves indicated the presence of more than one layer in the subsurface (a break in slope of the curve), reverse profiles were run by placing the geophone at the opposite end of the seismic line and repeating the procedure.

## Resistivity Sounding Field Procedures

12.  A resistivity sounding was run in the vicinity of the seismic line to complement the seismic interpretation. Nonconducting 200-ft, fiber-reinforced tapes were laid out in opposite directions from a center point and stakes were placed beyond 200 ft at the proper spacing out to 500-600 ft to mark the electrode stations. In a sounding array, the resistivity meter and cable reels are positioned at the center of the line and connected to the four electrodes by cables. The potential electrodes are emplaced at their initial close spacing, and apparent resistivity readings are taken for successively greater current electrode spacings (AB) until meter sensitivity is exceeded. The potential electrodes are then reimplanted at a greater spacing and the readings continued for increasingly greater current electrode spacings. Potential electrode spacings (MN) of 2, 30, and 70 ft were used in the soundings. The procedure is repeated until the electrode spacing becomes too large to achieve reliable meter readings. Figure 5 illustrates the basic features of a resistivity sounding.

13.  For each reading it is necessary to null any self potential developed between potential electrodes by means of a galvanometer dial on the instrument. Current is then applied to the circuit by means of the current switch on the instrument, and the resistance is measured by nulling out the galvanometer with a rheostat. The resistance value obtained is that used in the equations to calculate apparent resistivity. The values of apparent resistivity and the half current electrode spacing are then plotted on log-log graph paper for matching with the master curves. The scale of the field curve graph paper and that of the master curve must always b the same. High quality, dimensionally stable paper should be used. Interpretation of the curves yields the thickness (E) and true resistivity ($\rho$) of electrically contrasting subsurface layers. See Orellana and Mooney,[6] pages 21 and 22, Figures 8 and 9.

## Resistivity Profile Field Procedure

14. Wenner resistivity profiles were run to locate the lateral position of buried or obscured geological contacts. The four electrodes in a Wenner resistivity profile are maintained at constant and equal spacing for a given profile line. The entire electrode array is moved a constant distance along the line for each new apparent resistivity reading. Electrode spacing determines the depth of penetration of the survey. The depth of influence of the electrode array can be roughly estimated as between one and three times the electrode spacing. An electrode spacing of twice the expected target depth was used initially for most of the profiles run in this investigation. The electrode array was usually advanced a distance equal to the length of the array (three times the electrode spacing) for each successive measurement in a profile. Where more overlap was needed for more detail, the array was advanced a lesser distance, e.g., two times the electrode spacing. The apparent resistivity values were plotted as the ordinate on linear graph paper, with the center position of each measurement plotted as the abscissa, thus showing the change in apparent resistivity along the profile's traverse. Part III of this report demonstrates the interpretation of profile data. The profile requires more time to run than the sounding because the entire system must be moved along the traverse and reassembled for every three or four measurements, depending on the electrode spacing being used.

PART III:  TESTS AND RESULTS

## Old River Outflow Channel Site

Analysis of data

15.  The Old River field investigation was run parallel to the
outflow channel west of the Old River Control Structure, along a stretch
of shell road (Figure 6).  Figures 7 and 8 are a geologic map and cross
section of the area.  Field data stations, which are approximate, are
referred to the existing stationing along the channel, the latter
stationing being measured along the channel westward from the center of
the control structure.  A Wenner array resistivity profile was run first
from sta 45+50 (4550 ft west of center of structure) to sta 98+30.  The
electrodes were spaced 80 ft apart ("a" spacing) and the array was moved
240 ft ("d" spacing) with each measurement (see Figure 9).  The profile
was run on grass-covered ground between the road and the high brush
bordering the road right of way.  A Schlumberger array resistivity
sounding was then conducted in the vicinity of the clay plug, with the
center of the sounding at sta 71+10 (see Figure 5).  The maximum current
electrode spacing (AB) for the sounding was 1200 ft.  A second sounding
was run east of the mapped edge of the clay plug at sta 46+50.  The
maximum AB spacing achieved there was 1000 ft.

16.  Seismic traverses, using the single-channel enhancement unit,
were run first at sta 76+10 (sta 1 of Figure 6) and then at sta 46+30
(sta 2 of Figure 6) to complement the resistivity soundings.  One line
was run at sta 1, from sta 76+10 eastward to 75 ft.  Two lines were run
at sta 2, 300 ft to the west and 300 ft to the east.

17.  The resistivity profile was positioned to cross both sides of
the buried clay plug as mapped from borings and aerial photography
(Figure 7).  The electrode "a" spacing was maintained at 80 ft to assure
that the depth of influence was well within the clay plug.  Figure 10 is
the graph of the profile data.  A marked contrast in apparent resis-
tivity ($\rho$) values occurs between sta 79+10 and 57+50.  The relatively
uniform values of about 70+ ohm-ft within this zone differ substantially

12

from the values of 120+ ohm-ft to the east and west. It is clear from
the data of Figure 10 that a zone of low-resistivity material 20 to
80 ft deep was crossed by the array between sta 57+50 and 59+90 on the
east, and sta 76+70 and 79+10 on the west. The $\rho$ peaks exhibited on
the graph at sta 79+10 and 57+50 are characteristic of curves of pro-
files crossing contacts of zones of different resistivities. The peaks
are caused by anomalous apparent resistivity values measured as differ-
ent electrodes of the array cross the contact[9] (page 221, Figure 146B).
The contact between the zone of low resistivity (the clay plug) and the
high-resistivity material on either side is interpreted to be beneath
sta 58+70 and 77+90. The geologic cross section constructed from
previous borings in the survey area is shown in Figure 8 (see Figure 6
for locations of these borings). The clay plug contacts as determined
by the resistivity data are shown on the cross section in their true
stationing positions and as they would appear projected into the line of
borings parallel to the trend of the mapped contacts. The position of
the eastern-most contact as interpreted from the resistivity profile
agrees very well with the mapped position. The interpreted position of
the western-most contact lies some 800 to 1000 ft east of the mapped
position. Control for mapping of the contact was primarily borings 12-C
and GS-28 (Figure 7) and aerial photo coverage. Boring 12-C does not
show a great thickness of the fat clay characteristic of the clay plug,
and penetrates substratum sands at a depth relatively shallow compared
to boring 10-C. The thinner portion of fat clay in boring 12-C probably
indicates that the boring lies near the western edge of the plug. The
position of the contact as inferred from the resistivity data, when
projected into the line of borings parallel to the trend of the plug,
lies very near boring 12-C. This, and the excellent quality of the
field curve, indicates that the contact may actually lie to the east of
its presently mapped position.

18. Boring GS-28 (Figures 6, 7, and 8) penetrated silty sands and
sands indicative of point bar at a relatively shallow depth lying to the
west of the clay plug. The resistivity profile data show an increase in
apparent resistivities to the west, which could be explained by the

13

presence of more resistive materials such as coarse point bar deposits. The borings to the east of the plug (e.g., boring 8-C) pass through fat clay at 30 to 40 ft (probably backswamp) and enter substratum sands at around 40 ft. Apparent resistivities east of the contact indicate materials similar to those west of the plug, and probably represent the shallow substratum sands. The presence of relatively shallow, high-resistance (electrically contrasting) materials bordering the conductive clay plug makes it possible to recognize the plug's presence and determine its position.

19. A resistivity sounding was run within the clay plug zone (sta 71+10) to attempt to determine the thickness of overlying fill, the water table depth, and the depth to the base of the plug. Figure 11 is the graph of apparent resistivity versus the half current electrode spacing ($L$). A smooth curve must be obtained in a resistivity sounding conducted in an area that is free of lateral inhomogeneity (Reference 4, page 37). Sharp breaks in the curve are caused by the presence of lateral changes in the earth. The curve in Figure 11 exhibits a good three-layer curve out to a total AB spacing of 120 ft ($L = 60$ ft). A sharp break is then indicated and a somewhat poorer curve is described out to $L = 600$ ft. The interpretation of this curve is limited to the smooth portion on the left, and indicates a very thin (1.3 ft) surface layer of about 50 ohm-ft underlain by about 13 ft of conductive (19 ohm-ft) material, and a more highly resistive material of about 120 ohm-ft below that. The depth of influence for the sounding was probably too shallow to detect the clay plug material. A low true resistivity was expected for the clay plug. Had the field curve not been disrupted by the apparent lateral change beyond $L = 60$ ft, there might have been sufficient penetration to detect the clay plug.

20. A second sounding was conducted east of the contact, at sta 46+30. A fairly smooth five-layer curve was produced out to $L = 500$ ft (Figure 12). The auxiliary point method of curve interpretation becomes less accurate when used on field curves of more than four layers (Reference 6, page 33). Therefore, an interpretation was made using only the upper four-layer portion of the curve. The interpretation

14

indicates about 2-1/2 ft of 22-ohm-ft material at the surface, then
53-ohm-ft material down to about the 14-ft depth; 20-ohm-ft material
below that down to 37 ft; and a stratum of relatively high (114 ohm-ft)
material below that. The position of the sounding is close to the line
of borings between borings 8-C and G3-15 (see Figure 6). The base of
the fat clays (backswamp?) between the two borings would be by inter-
polation about +16 ft mean sea level (msl). The sounding indicates a
change from conductive material above to more resistive material below
at about +20 ft msl. The presence of at least a fifth layer of lower
resistivity below that, however, reduces the confidence in correlating
the sounding with the borings. The reason is that one would expect,
from the borings, a general increase in resistivity with depth at this
station. The electrical soundings did not produce sufficient depth of
penetration to be of significance at this site. Lateral variations in
earth materials at sta 1, complexity of the subsurface materials at
relatively shallow depths at sta 2, and inability to detect the very low
potential differences on the instrument at large L distances contributed
to the inadequacy of the soundings.

21. Seismic refraction surveys were run near each of the two
sounding stations. The first was run from sta 1 (sta 71+10) eastward
75 ft (Figure 13). Good signals were obtained out to 75 ft but signals
beyond that were too poor to be read with confidence. Figure 14
illustrates the form and relative quality of the seismograph signals.
Travel times noted are for first arrivals. A gap in the curve occurred
between hammer stations 45 and 50 ft, and the slope reverted to that of
a lower velocity material. The curve in Figure 13 describes a three-
layer subsurface with a lateral change occurring east of hammer station
40 ft at about the depth of the third layer. Figure 15 shows the cross
sections that could be inferred from the seismic and resistivity data at
sta 1. A similar subsurface structure with its corresponding travel
time-distance graph is illustrated in Mooney[5], Chapter 15, Figure C.2.b.
The 4000-ft/sec compressional wave velocity for the lower layer could be
indicative of a water-saturated sand. Interpretation of the third layer
as a sand would also agree with the resistivity section, which shows a

15

relatively more resistive unit below about 13-ft depth. The third layer
described here could be explained as a sand lens within the clay plug.
The lateral change, exhibited in both the resistivity and the seismic
lines, might then represent the transition into the clay portion of the
plug. The unit directly above the third layer with its base at about 11
and 13 ft in the seismic and resistivity cross sections, respectively,
may represent natural levee deposits which blanket much of the area
around the Old River outflow channel.

22. Excellent signals were received out to 500 ft on the two
seismic lines run at sta 2 (Figures 16 and 17). All data points lie on
or very near a single line passing through the origin. The inverse
slopes of the two lines are essentially identical, 1128 ft/sec and
1132 ft/sec. Two interpretations are offered for the data: (a) the
data represent a single, thick, low-velocity surface layer extending to
a depth of at least 116 ft, and (b) the data represent a low-velocity
surface layer of undetermined thickness underlain by a thick lower
velocity intermediate layer that masks the deeper subsurface materials.
The velocity of water-saturated sediments can be said to range between
3000 and 6000 ft/sec. The water table should have been encountered at
about 20-30 ft depth (approximate elevation of the water in the outflow
channel). For that reason the first interpretation, that of a low-
velocity material 116 ft thick, is untenable. The second interpretation
is the simplest and most logical explanation. Figure 18 illustrates how
the graph of sta 2 could be produced by the presence of a thick, low-
velocity layer below the surface layer. The direct wave, traveling at,
in this case, 1130 ft/sec, normally is recorded as a first arrival until
the refracted signal from the faster layer at depth overtakes it. The
presence of a low-velocity $V_2$ zone between the $V_1$ and $V_3$ layers,
however, refracts the seismic wave downward and in effect lengthens the
path and slows the wave so that even at great geophone-impact distances
the direct wave continues to arrive before the refracted wave. A single
slope is thus produced on the time-distance curve. The low velocity $V_2$
zone possibly represents the backswamp fat clays shown in borings 8-C
and GS-15, Figure 8. Entrapped gas in the backswamp material would

16

lower its effective velocity. Normally, forward and reversed lines are run for each seismic station, but because only the direct wave was received, a reverse line was unnecessary.

## Summary of results

23. The resistivity profile was apparently very effective in locating the position of the abandoned channel clay plug. A more precise definition of the contacts could be achieved by overlapping the measurements by one or two "a" spacings and obtaining a greater number of data points. The resistivity soundings failed to achieve sufficient depth to be of practical significance in a geological study. The cross section interpreted from the sounding in the clay plug correlated fairly well with the seismic refraction data there but neither was deep enough to warrant confidence in geologic interpretation of the subsurface. Similarly, neither seismic refraction line adequately pictured the subsurface structure, probably because of complex near-surface geology and variations in earth materials laterally.

## Lock and Dam No. 3 Site, Red River

### Analysis of data

24. The field investigation at Lock and Dam No. 3 was conducted along an unimproved road running northwest from the river (see Figure 19). Figure 20 is a geologic map of the area and Figure 21 shows the logs of four borings near the road. A resistivity profile was made from the river end of the road (sta 0), a distance of 1530 ft up the road. An "a" spacing of 20 ft and "d" spacing of 60 ft were used. Electrical soundings were conducted at about 720 ft (sta 1) up the road from sta 0, and at about one mile (sta 2) up the road (Figure 19). The sta 1 sounding was carried out to an AB distance of 800 ft. The sta 2 sounding was carried out to an AB of 400 ft. Reversed seismic lines were run east and west from sta 1 with the geophone set at sta 1. One reversed seismic line was run at sta 2 eastward.

25. The resistivity profile was started near the riverbank and worked up the road in hopes of detecting the point bar-backswamp and backswamp-terrace contacts. Since the contacts were assumed to be near

17

the surface, an "a" spacing of only 20 ft was used. Figure 22 is the graph of the profile data. The traverse runs from right to left on the graph. The graph is too erratic for interpretation. A profile must exhibit a segment of uniform values before a contact may be confidently picked, but the profile shown here is a series of peaks and troughs with few or no uniform apparent resistivity segments.

26. The electrical sounding at sta 1 is graphed in Figure 23. The field curve is fairly smooth out to L = 100 ft, except for two cusps at 15 and 50 ft. Cusps can be caused by an anomalous material near one of the electrodes or current leakage in the cables (Zohdy[4], page 37). Current leakage problems were experienced at this site and were possibly the cause of the cusps. A substantial amount of smoothing of the curve was necessary, evident on the field curve, and lowers the confidence of the interpretation of the curve. A fair curve match was made with a three-layer master curve, but a better fit was achieved using auxiliary curves. The interpreted section shows 11 ft of 32 ohm-ft material underlain by 25 ft of 112 ohm-ft material, underlain by an undetermined thickness of 23 ohm-ft material. The elevation of sta 1 is approximately 105 ft (see Figure 19). The nearest borehole is over 1700 ft to the north of sta 1 (Figure 19), and it is not possible to correlate the sounding with either boring 3-22G or 3-1G (Figure 21). The sounding was not deep enough to detect the Pleistocene-Tertiary contact, the elevation of which should be much as shown in Figure 21.

27. The sounding at sta 2 was hindered by curves in the road and changing ground elevation with increase in electrode spacing. Therefore, the line was run to an AB spacing of only 400 ft. The curve was relatively smooth out to L = 100 ft, but considerable smoothing was necessary beyond that. A four-layer model was interpreted by means of auxiliary curves as shown in Figure 24. The interpretation yielded a relatively high-resistivity subsurface, which perhaps would be expected in the granular terrace deposits in which the sounding was run. The interpreted cross section is 1075 ohm-ft material from the surface down to 4 ft, then 415 ohm-ft down to 9 ft, then 2400 ohm-ft material to 26 ft, and below that material of 1075 ohm-ft. Sta 2 is about 300 ft

18

from boring 3-240, shows a thick sequence of silty sand below about 16-ft depth, and one would expect an increase in resistivity below 16 ft as dry coarser materials are encountered. The position of the water table is not indicated in the boring logs. The elevation of the ridges at sta 2, as shown in Figure 19, above the intermittent stream and the swamp, infers a deep water table (below elevation +100 ft msl), so that the assumption can be made that the terrace material is dry down to at least 20-ft depth. The sounding does not correlate with the boring. Again, not enough depth was reached to detect the terrace-Tertiary contact at its depth of about 90 ft.

28. Two reversed seismic lines were run at sta 1, one east to 260 ft and one west to 230 ft. Figure 25 shows the result of the west to east line. Two layers are indicated: a 1050-ft/sec upper layer about 10 ft thick, and a 5400-ft/sec layer below that. A very slight dip to the west ( 1 deg) is indicated by the data. Figure 26 shows the curves for the east to west line. These data indicate a similar subsurface with a somewhat faster surface layer (1667 ft/sec) and an underlying material of about the same velocity as that of the other line (5658 ft/sec). A dip of a little over 3 deg to the west is indicated. The cross section inferred from the two lines is shown in Figure 27. There is a discrepancy between the two lines concerning the depth to the high-velocity layer. The discrepancy of about 7 ft may be caused by a gradual change in surface layer velocity between ends of the two seismic lines. A curved slope of the $V_1$ layer is noted in both lines near the central point (sta 1). Such a slope is characteristic of a uniform increase in velocity with depth, for example by overburden consolidation. These variances in $V_1$ could produce errors in the calculations of depths because the single value chosen for $V_1$ is used in the depth equations (see Figures 25 and 26). A dashed line has been drawn on Figure 23 as the averaged depth to the top of the $V_2$ layer. The structure could be interpreted as a 15- to 20-ft layer of soil and weathered terrace deposits underlain by unweathered sandy terrace deposits. The electrical sounding (Figure 23) shows fair agreement with

19

this interpretation--the 11-ft-thick, 32 ohm-ft upper zone representing the clayey weathered porti and the 112 ohm-ft material below representing the sandy unweathered material.

29. A reversed seismic line was run at sta 2, west to east, a distance of 180 ft. Signals beyond that distance were too weak. A two-layered subsurface was indicated by the time-distance plots (Figure 28), the contact dipping a little over 1 deg to the west. The data represent a typical two-layer curve except for the apparent time delay (gap) in the arrival of the $V_2$ signals, at hammer stations 60 and 105 ft. The arrival time gap is difficult to explain. The shape of the graph is similar to that for a buried step, as illustrated in Mooney,[5] Chapter 15, Figure C-7a. The gap in Figure 28, however, occurs concurrently with the break in slope, and indicates an anomalously later arrival on both forward and reversed seismic lines, and therefore does not fit a buried step interpretation.

30. The inferred cross section (Figure 29) was constructed from the data neglecting the time gap. Comparison of the seismic data cross section with boring 3-24G (Figure 21), and with the electrical sounding (Figure 24), places the $V_1$-$V_2$ contact midway within the silty sand of the boring and near the base of the 2400 ohm-ft layer of the sounding. One explanation consistent with both sets of data is that the water table was encountered at a depth of about 26 ft (sounding data) to 32 ft (seismic data). The presence of groundwater in the sediments would both lower the resistivity of the material and increase its velocity to about that indicated by $V_2$ (5127 ft/sec).

## Summary of results

31. It was hoped that the geophysical data would detect the contact of the Pleistocene terrace deposits on the Tertiary bedrock below and that the lithologies of the two units could be predicted from velocity and resistivity values. The contact was too deep for the low-energy type surveys run, however, and only a relatively shallow section was investigated. The seismic and electrical data were sufficiently correlative that an interpretation could be made consistent with both sets of data and somewhat consistent with the limited borehole data.

32. An electrical sounding and a seismic refraction line were attempted at this site although it was felt beforehand that the presence of a steel cutoff wall within the levee would cause anomalous data. The surveys were run parallel to the levee, between the east levee and the road (Jourdan Road), from sta 1 of Figure 30. The sounding was run to a maximum of 160 ft (AB spacing). The field curve (Figure 31) shows a continuous drop in apparent resistivities with increasing electrode spacing. Meter readings were much too low beyond 160 ft to be recorded with confidence. The rapid fall-off of values and the extremely low resistivity values obtained at wide electrode spacings were probably caused by deflection of the current field by the buried sheet pile cutoff wall, which would be highly conductive. As the current electrodes were moved farther apart from the measuring (potential) electrodes, the effect of the conductive wall would become more and more apparent.

33. A seismic line was run south from sta 1 (Figure 30) a distance of 380 ft. An apparent single-layer curve similar to that of sta 1 of the Old River site survey was obtained as shown in Figure 32. The 1125-ft/sec velocity for the single layer indicated in Figure 32 is far lower than the velocity that would be expected for the steel cutoff wall. It must be assumed, therefore, that the velocity is that of the ground, and that, as in the Old River survey, a low-velocity material underlies the surface layer in sufficient thickness and of sufficiently low velocity that it masks any higher velocity material below. Marsh and swamp deposits irregularly overlie the buried beach (Figure 33). The possible presence within these deposits of organic materials with entrapped gases would explain the existence of a low-velocity zone beneath the levee fill surface layer. Since an alternate site was available for investigation of the buried beach, no further attempts were made at the Inner Harbor Canal site.

21

## Metairie Outfall Canal Site, New Orleans

### Analysis of data

34. Seismic lines were run atop and at the base of the levee along the west side of the Metairie Outfall Canal. Figure 34 is a geologic cross section parallel to the canal and about 2300 ft east. One electrical sounding was run along the top of the levee, and a resistivity profile was run along the top of the levee a distance of about 4400 ft. The seismic lines were run from sta 1 (Figure 35) north to south atop the levee, and south to north at the base of the levee. Data points for the seismic line run atop the levee (Figure 36) were erratic beyond about 45 ft and only the surface layer could be interpreted with any accuracy; it showed a velocity of 1140 ft./sec. The depth to the second layer ($V_2$ = 3883 ft/sec) was computed as 16.8 ft (Figure 36) but little confidence should be placed on that value. The second seismic line was run at the base of the levee to attempt to obtain better second-layer data points. The line was run a distance of 200 ft from sta 1 north. The data for this line were much better (Figure 37). Two layers are indicated: one 9.2 ft thick with a velocity of 1124 ft/sec, and one of undetermined thickness at a velocity of from 3300 to 3900 ft/sec. A break in the slope of layer $V_2$ occurs at about 100 ft on the line. It indicates that the signals from this layer arrived earlier beyond 100 ft. This feature is best explained by the existence of a buried step, rising to the north, between layer $V_1$ and $V_2$ (see Mooney[5], Chapter 15, Figure C-7b). The geological interpretation of this data is discussed below.

35. A Wenner resistivity profile was run from sta 2 atop the levee (Figure 35) just south of I-10, a distance of about 4400 ft south. An "a" spacing of 80 ft and a "d" spacing of 160 ft (a two-electrode overlap) were used. A graph of the profile is shown in Figure 38. There is a gap in the data from 2200 ft to 3400 ft in which no measurements could be taken because of a railroad crossing and canal pumping station. Low, fairly constant apparent resistivities were measured south of 2000 ft; resistivities rose slowly north of 2000 ft and

sharply north of 1200 ft. Analysis of the profile data is included below with the discussion of the seismic results.

36. The resistivity sounding was run at sta 1 to an "L" spacing of 300 ft. Its field curve (Figure 39) shows a general decrease in resistivity with depth with an intermediate layer of higher resistivity. The curve could not be interpreted with the curve matching technique although two-layer and auxiliary curves were consulted for the most conservative approach. The rather sharp peak in the slope of the field curve at L = 80 ft may be caused by the limited lateral extent of a subsurface layer (Zohdy[4], page 40). The shape of the field curve indicates complexity in the subsurface. Figure 34 is a geologic cross section reconstructed from borings along Pontchartrain Boulevard from Lake Pontchartrain south to the Mississippi River. The main feature of the cross section is the near-surface buried beach between the 5,000- and 22,000-ft grid lines. The cross section indicates the complexity of the subsurface in the vicinity of the buried beach. The positions of sta 1 and 2, and the profile line, are shown projected into the geologic cross section parallel to the trend of the buried beach, as determined from an unpublished contour map of the top of the buried beach.

Geologic interpretation of data

37. The thickest portion of the buried beach runs from about the position of sta 1 northward beyond sta 2 (see Figure 34). South of sta 1 the beach sand thins so that the upper part is replaced by pro-delta clays. There is a thin (about 5 ft) marsh deposit overlying the beach and prodelta clay near sta 1 and 2. Probably less than 5 ft of surface fill exists in this area. The south-north seismic line at the base of the levee indicates a material of velocity of 3333 ft/sec at a depth of about 9 ft (Figure 37). That depth conforms well with the top of the thick portion of the buried beach. Therefore, the 3333-ft/sec layer is believed to be the buried beach. The buried step encountered in the seismic line (Figure 37) possibly represents an ancient beach scarp or terrace.

23

38.  Figure 34 shows the position of the resistivity profile with respect to the geologic cross section.  It is apparent from the field graph of the profile (Figure 38) that, at the depth of influence of the electrode array ("a" of 80 ft), a subsurface of relatively low resistivity was encountered in the southern two-thirds of the profile.  This material is inferred to be principally the prodelte lays to the south of the thick upper portion of the buried beach.  The sharp rise in the profile's graph from about 1200 ft northward (Figure 38) probably represents the influence of the thick, shallow portion of the coarse beach deposits.  The edge of this thickest part of the buried beach is inferred to be at the 1160-ft station on the profile, in good agreement with the geologic cross section (Figure 34).  The gradual rise in the curve between 2200 and 1240 ft is probably caused by a gradual thickening of the resistive beach at the expense of the conductive prodelta clay.

39.  The seismic refraction and resistivity profile surveys were considered successful in detecting and delineating the southern position of the buried beach, although boring data obviously were needed to make the liberal interpretations presented above.  The electrical sounding again failed to give usable data, attributable probably to the complexity of the subsurface deposits.

## Nine Mile Point, New Orleans

40.  Figure 40 is a general geologic map of the New Orleans area, and shows the approximate position of the point bar material on Nine Mile Point.  A resistivity profile was run from the vicinity of State Highway 18 northward about 3700 ft along the edge of the railroad grade construction on Nine Mile Point (see Figure 41).  An "a" spacing of 80 ft and a "d" spacing of 240 ft were used.  Reversed seismic lines and electrical soundings were run at two stations and a seismic traverse and sounding were attempted at a third.

41.  The purpose of the resistivity profile was to locate the contact between point bar materials on the north and backswamp deposits on

24

the south. The field curve for the profile is shown in Figure 42. Low apparent resistivity values were obtained in the southern half of the profile, indicating conductive subsurface there. The values rose sharply from about 2000 ft northward and were still rising when the profile was terminated. The presence of heavy woods and a canal prevented continuation of the profile to the north. The low resistivity values are inferred to represent the conductive backswamp clays and the higher values the coarser point bar materials. Ideally the curve would have leveled off to the north at a value of around 40 or 50 ohm-ft. Because the profile could not be extended far enough in that direction, the interpretation must be made without benefit of the complete curve. The contact is inferred at the 3000-ft position of the profile (Figure 42), about midway on the rising portion of the field curve. Its position is shown marked in Figure 41. The approximate position of the contact has been mapped previously from aerial photography (Figure 40). The mapped contact is shown dashed on Figure 41 and lies about 1300 ft north of the position of the contact as inferred in this report. The resistivity-inferred position of the contact could be in error by several hundred feet (too far south) because a peak on the field curve was never reached. The mapped position, however, may also be in error because of the lack of boring control in this area. It is felt that the profiling technique was effective in detecting the presence and influence of the point bar as the profile moved northward, but the lack of sufficient access length prevented a concise and complete interpretation.

42. Survey stations 1, 2, and 3 are shown in Figure 41. A seismic refraction line was run northward from sta 1, a distance of 140 ft, and the line was reversed from 90 ft back (Figure 43). Seismic signals were relatively poor at the Nine Mile Point site, probably because of attenuation caused by the generally soft clayey upper portion of the soil. Accordingly, shorter lines were run and less depth of penetration was achieved. Interpretation of the reversed portion of the seismic line indicates two layers, the upper very slow at 700 ft/sec, the lower at a depth of about 6-10 ft with a velocity of 2800 ft/sec. The forward or south to north line run out to 140 ft indicates a

25

possible third layer. Using the intercept time and the slope from the
four data points received for the layer, a velocity of about 7700 ft/sec
and a depth of 40 ft were computed for this layer (see Figure 43). Such
a velocity is higher than that expected for unconsolidated point bar
deposits. Also, the layer is too deep. No geologic interpretation is
offered here for the apparent third layer because of the erratic nature
of the data points beyond 90 ft.

43. The resistivity sounding was run at sta 1 to a total AP
electrode spacing of 1000 ft. Readings on the instrument scale were
very low, however, and usable measurements were made only out to 160 ft
(L = 80 ft). The limited curve (Figure 44) indicates a three-layer
subsurface with generally low resistivity values. The depth of influ-
ence of the sounding is too shallow to warrant attempting a geological
interpretation.

44. A reversed seismic line was run south from sta 2, a distance
of 100 ft (Figure 45). The data beyond 70 ft were those of a slower
velocity material, and it was assumed that a lateral change occurred
beyond 70 ft. Therefore, the line was reversed only from 60 ft back.
The interpretation was similar to that of sta 1: a low-velocity layer
(973 ft/sec) down to about 10 ft, and a higher velocity material
(3049 ft/sec) below that. The seismic data for the two stations are
consistent enough that something about the shallow geology there can be
inferred. The low velocity, 10-ft-thick upper layer may represent the
natural levee blanketing the point bar-backswamp materials, with satu-
rated r diments beneath; or it may represent the nonsaturated soil
overlying the deeper saturated sediments.

45. The field curve and interpretation of the electrical sounding
run at sta 2 are presented in Figure 46. A smooth curve could be drawn
out to L = 100 ft, which represented a depth of influence of less than
20 ft. There  > obvious correlation between the sounding interpre-
tation and that of the seismic line. A seismic line and resistivity
sounding were attempted at sta 3 but were unproductive. Field curves
for the respective surveys are shown in Figures 47 and 48.

26

# PART IV: CONCLUSIONS AND RECOMMENDATIONS

46.  The hammer seismic and surface resistivity exploration
methods show some promise for use in the alluvial terrain of the lower
Mississippi Valley.  This study indicates that their use is limited to
relatively shallow (less than 100 ft) depths and that they rarely can be
expected to be used with equal success at the same site.  Conversely,
the seismic and resistivity techniques should be used in conjunction
with each other and with existing boring and outcrop data to obtain
complementary data for the best possible interpretation of the
subsurface.

47.  The best results were obtained with the resistivity profile
surveys.  The profiles were very effective in most situations in
locating subsurface contacts and bodies of anomalous geologic materials.
Approximate depth of interest (penetration) can easily be controlled by
adjusting the electrode spacing.  One possible limitation to the appli-
cation of the profile would be lack of sufficient line length in which
to run the survey, especially when using a large electrode spacing.

48.  The resistivity soundings delineated very shallow electrical
discontinuities such as soil layers and moisture variances, but were
ineffective in attaining sufficient depth to allow construction of
substantial geologic sections.  The probable causes of the soundings'
ineffectiveness are complex subsurface structures in some of the test
areas, lateral variations in electrical properties in subsurface
materials of many of the sites, and insensitivity of the instrument at
large electrode (L) spacings.

49.  The hammer seismic device was unable to achieve adequate
depth of penetration in the unconsolidated deposits encountered at many
of the sites.  This is attributed to severe attenuation of the hammer
impact by the loose, sometimes dry near-surface materials.  Refinements,
however, are being made in portable hammer seismic equipment, such as
the development of multi-channel, signal-enhancement units.  Use of the
improved units may permit more efficient, higher resolution surveys to
be conducted.  The seismic data were useful in some situations in

27

correlating shallow data obtained in the other surveys. The hammer
seismic equipment performed best in the upland terrain of the Red River
Lock and Dam No. 3 site, probably because of the higher consolidation of
the earth materials, and in the Metairie Outfall Canal area, where the
saturated sands of the buried beach deposit transmitted the low-energy
seismic signals better. Another apparent problem with the hammer
seismic surveys was the masking of deeper materials by a low-velocity
intermediate layer, as at the Old River and Inner Harbor Navigation
Canal sites. The likely presence of low-velocity intermediate zones
should be recognized in using the refraction seismic method in alluvial
deposits.

50. Man-made structures, in this case a steel sheet pile cutoff
wall, proved to be a major obstacle at one site (Inner Harbor Navigation
Canal) and hampered surveys at another (Metairie Outfall Canal). Such
features are expected in urban areas but will have to be avoided
wherever possible. Where subsurface features of sufficient areal extent
are being investigated, alternate survey sites should be selected to
avoid troublesome man-made structures that may be present.

51. None of the three methods discussed can yield unique inter-
pretations without substantial subsurface truth data such as exploration
trenches or drill hole data. These data are needed to establish
lithologies, resolve the equivalence (ambiguity of interpretation)
inherent in the resistivity methods, and develop a degree of confidence
in the surveyor's interpretations.

REFERENC. 3

1. Dobrin, M. B., "The Seismic Refraction Method," Introduction to
   Geophysical Prospecting, 2nd ed., McGraw-Hill, New York, 1960.

2. Redpath, B. B., "Seismic Refraction Exploration for Engineering
   Site Investigation," Technical Report E-73-4, August 1973, U. S.
   Army Engineer Waterways Experiment Station, Explosive Excavation
   Research Laboratory, Livermore, California.

3. Musgrave, A. W., Ed., "Interpretation Techniques for Refraction
   Work," Seismic Refraction Prospecting, The Society of Exploration
   Geophysicists, Tulsa, Oklahoma, 1967.

4. Zohdy, A. A. R., "Electrical Methods," in Techniques of Water-
   Resource Investigations of the United States Geological Survey,
   Chapter D1, "Application of Surface Geophysics to Ground Water
   Investigations," U. S. Government Printing Office, Washington,
   D. C., 1974.

5. Mooney, H. M., Handbook of Engineering Geophysics, Bison Instru-
   ments, Inc., Minneapolis, 1973.

6. Orellana, E. and Mooney, H. M., Master Tables and Curves for
   Vertical Electrical Sounding, Interciencia, Madrid, 1966.

7. Keller, G. V. and Frischknecht, F. C., Electrical Methods in
   Geophysical Prospecting, Pergamon Press, Oxford, 1966.

8. Dobrin, M. B., "Electrical Prospecting Methods," Introduction to
   Geophysical Prospecting, 2nd ed., McGraw-Hill, New York, 1960.

9. Van Nostrand, R. G. and Cook, K. L., "Interpretation of Resistivity
   Data," U. S. Geological Survey Prof. Paper 499, 1966, U. S. Govern-
   ment Printing Office, Washington, D. C.

10. Saucier, R. T., "Geological Investigation of the Boeuf-Tensas
    Basin," Technical Report No. 3-757, February 1967, U. S. Army
    Engineer Waterways Experiment Station, Vicksburg, Mississippi.

11. U. S. Army Engineer Waterways Experiment Station, "Geologic
    Conditions at the Low-Sill Structure, Old River Control Site,"
    Miscellaneous Paper No. 3-126, May 1955, Vicksburg, Mississippi.

12. Mississippi River Commission, "Mississippi River and Tributaries,
    Old River Control, Outflow Channel," Design Memorandum No. 6A,
    Vicksburg, Mississippi.

29

13. U. S. Army Engineer Waterways Experiment Station, "Geology of the Mississippi River Deltaic Plain, Southeastern Loui: iana," Technical Report No. 3-483, Vol 2, July 1958, Vicksburg, Mississippi.

14. U. S. Army Engineer Waterways Experiment Station, "Pleistocene Sediments of the New Orleans-Lake Pontchartrain Area," Technical Report No. S-75-6, June 1975, Vicksburg, Mississippi.
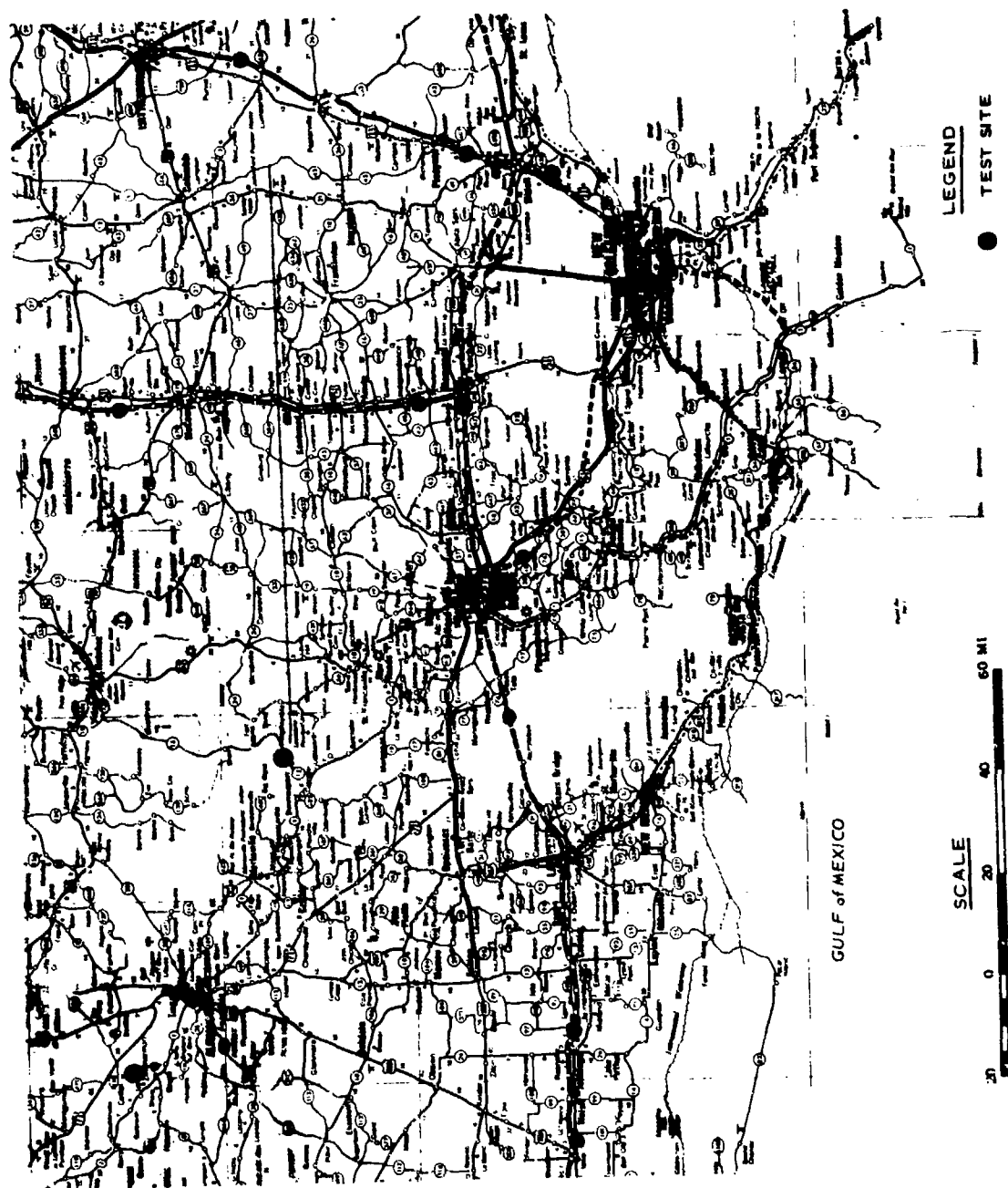
Figure 1. Locations of geophysical test sites
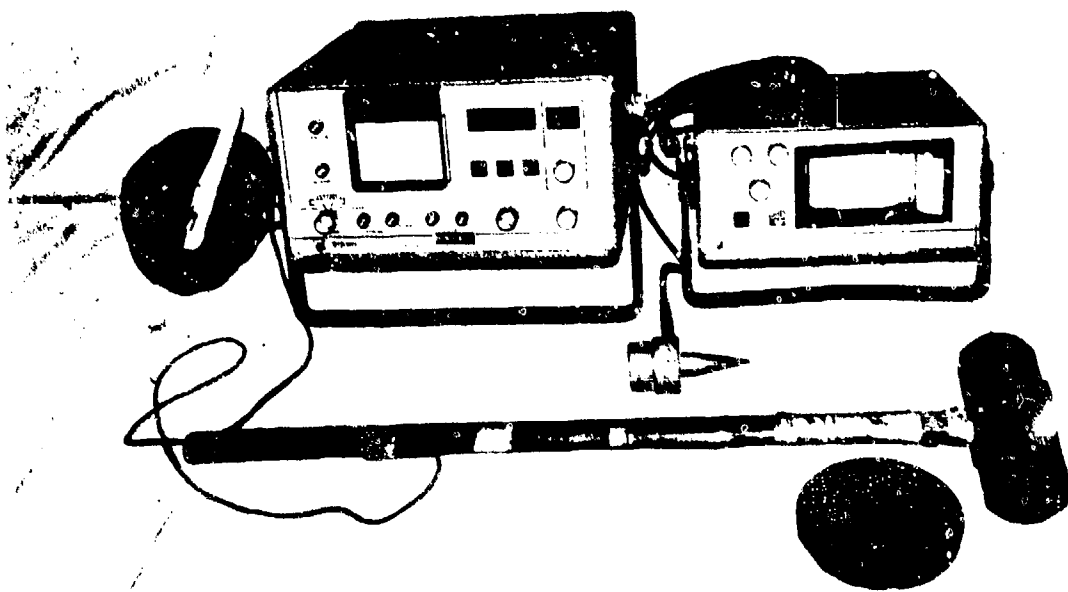
Figure 2. Bison Model 1575-B seismograph, strip chart
recorder, hammer, and striking plate.
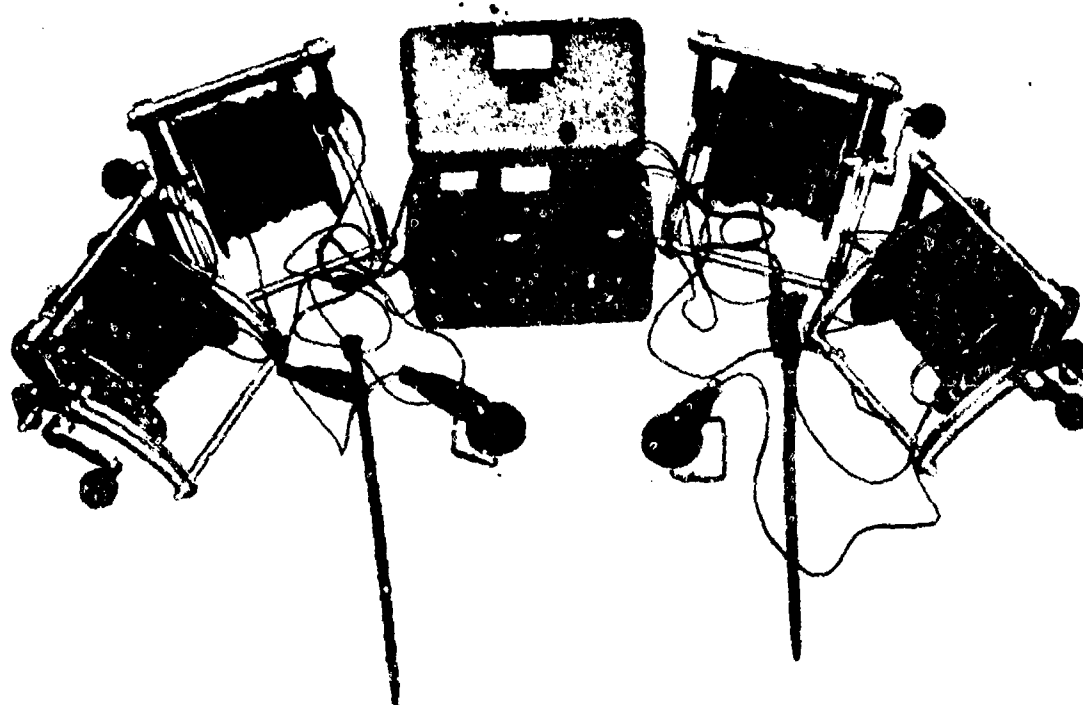
Figure 3. Keck Model IC-69 resistivity
meter, cable reels, and electrodes.
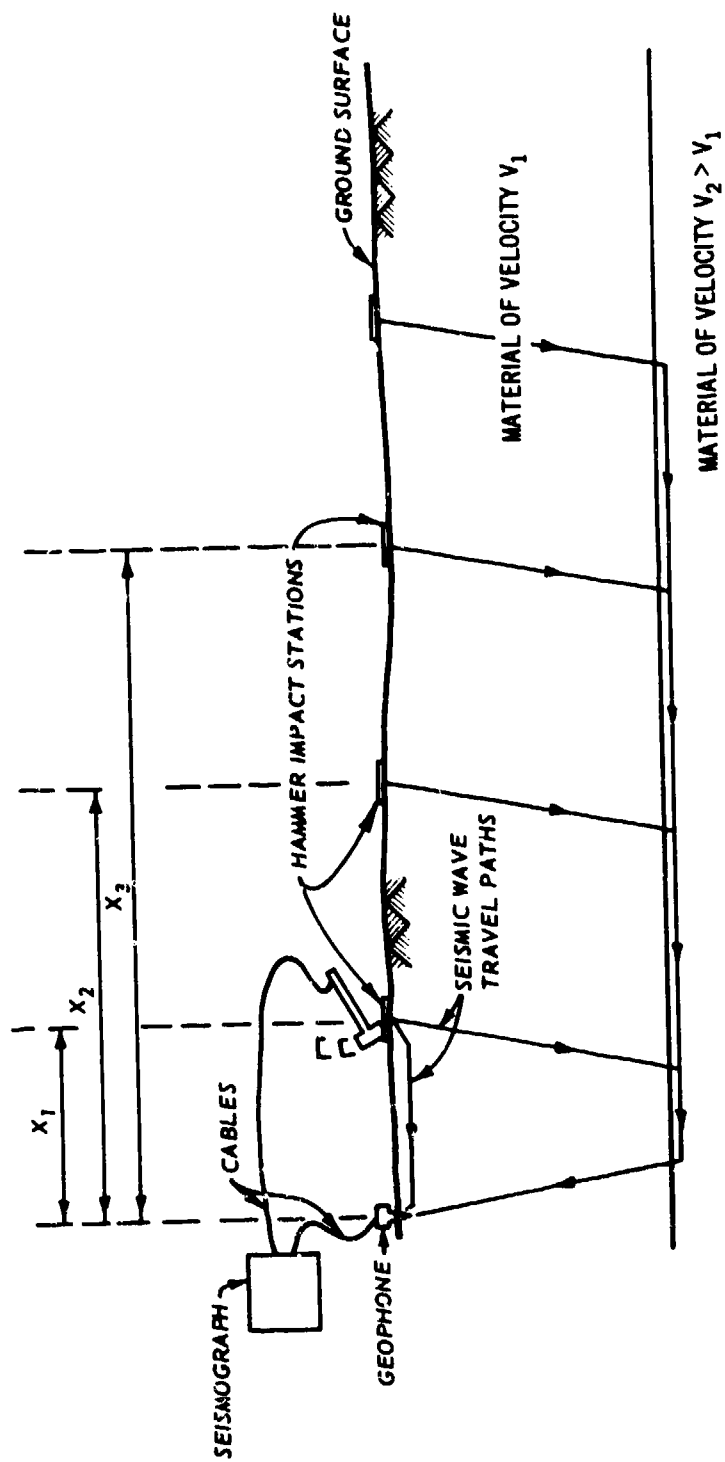
Figure 4. Basic features of typical hammer seismic refraction line
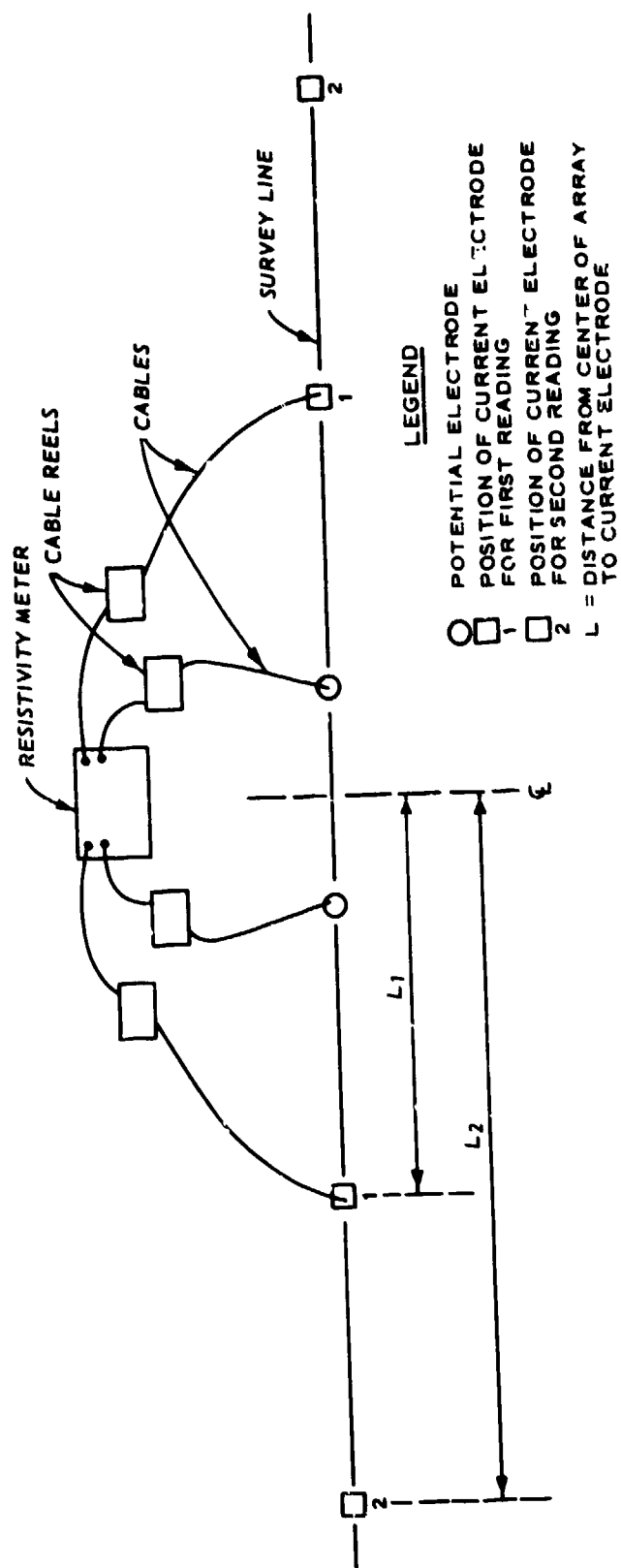
Figure 5. Basic features of typical resistivity sounding

SURVEY LINE

RESISTIVITY METER
CABLE REELS
CABLES

LEGEND

○ POTENTIAL ELECTRODE

☐1 POSITION OF CURRENT ELECTRODE
FOR FIRST READING

☐2 POSITION OF CURRENT ELECTRODE
FOR SECOND READING

L = DISTANCE FROM CENTER OF ARRAY
TO CURRENT ELECTRODE
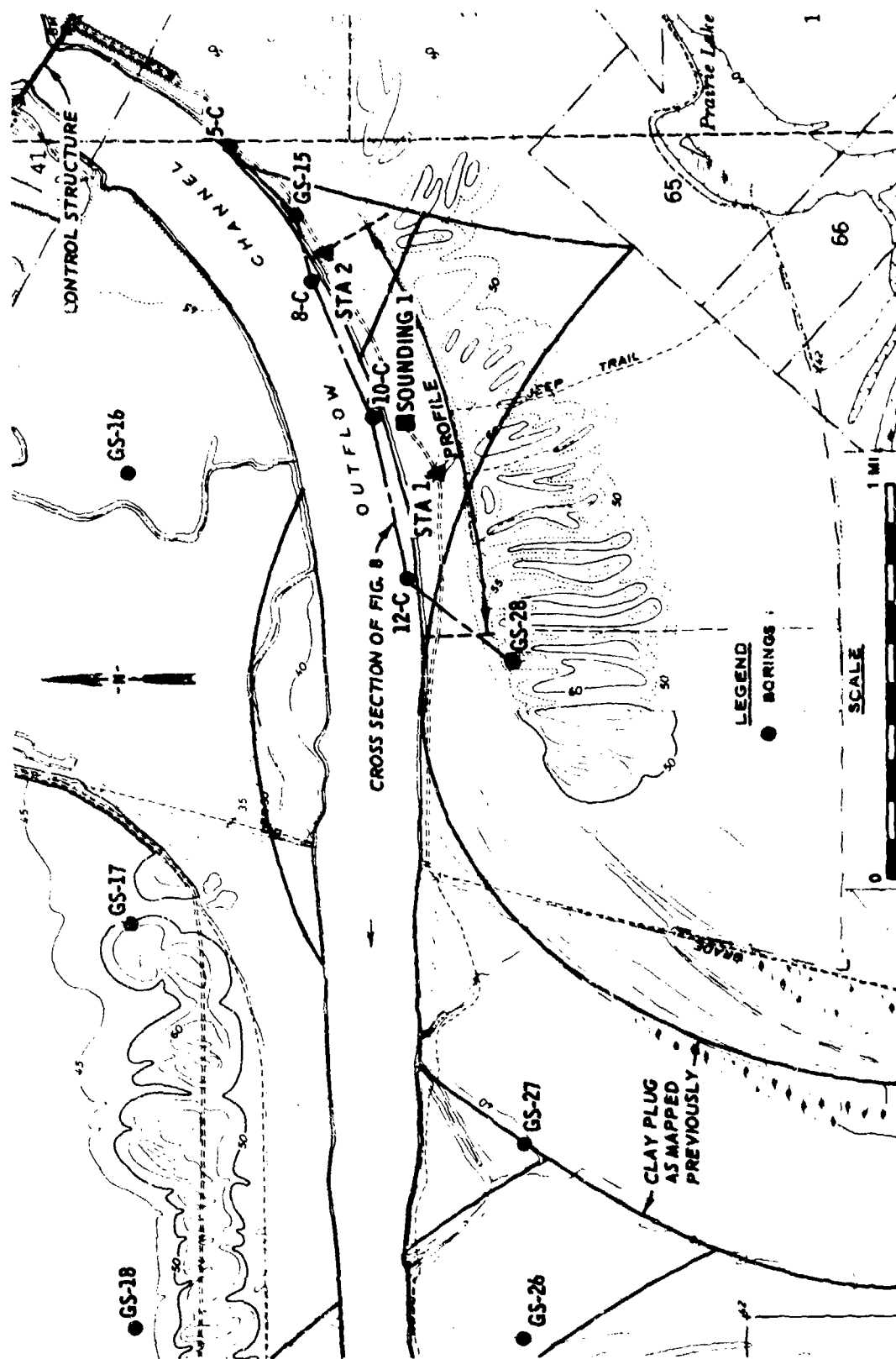
Figure 6. Map of Old River site
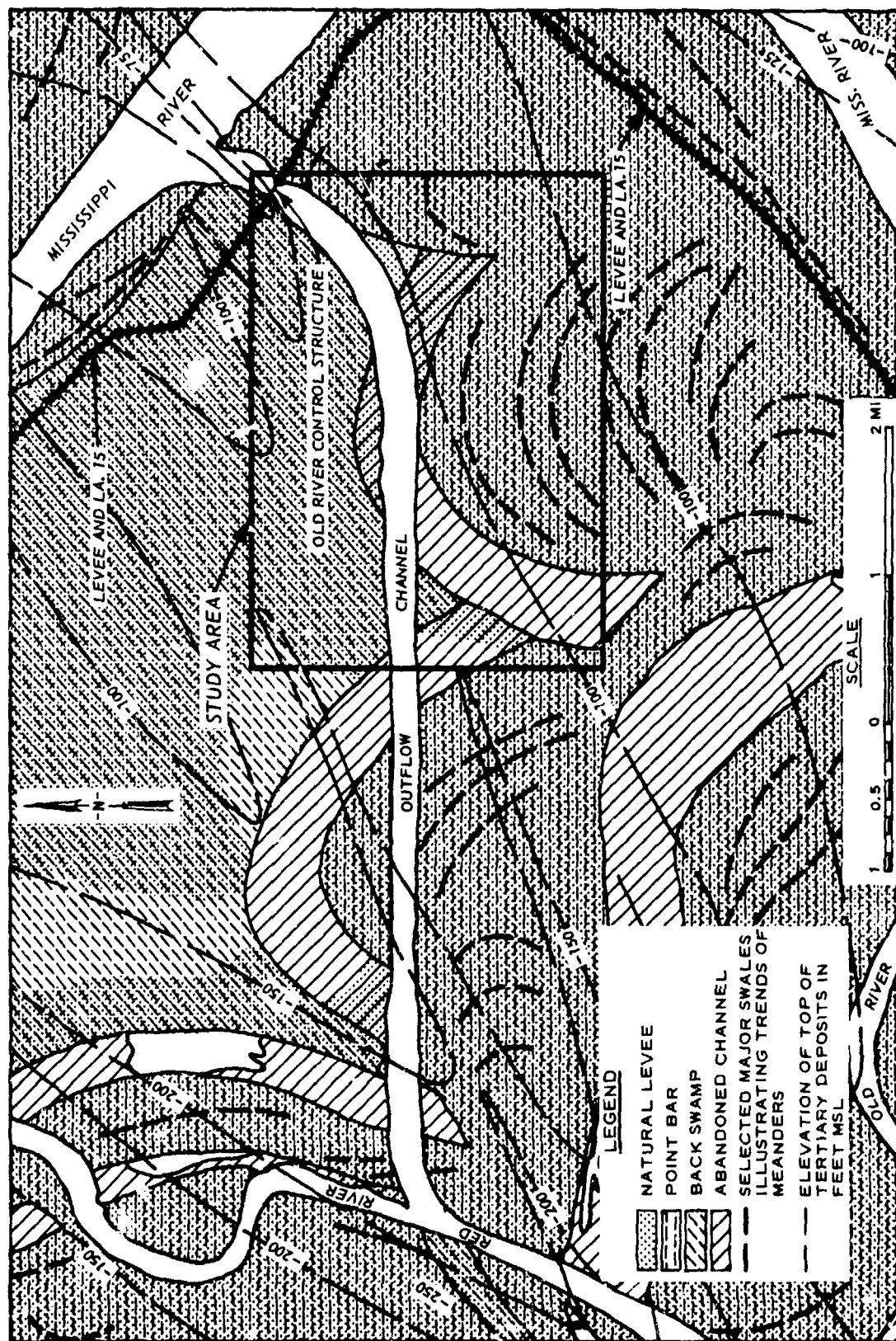
Figure 7. Geologic map, Old River outflow channel area
(from Reference 10)

WEST

ELEVATION, FT MSL

80

40

0

-40

-80

GS-28

POINT BAR

12-C

BEND IN SECTION

RESISTIVITY CONTACT PROJECTED INTO
PARALLEL TO MAPPED CONTACT

CLAY PLUG CONTACT BY
RESISTIVITY PROFILE

CLAY PLUG CON
INFERRED FROM

APPROXIMATE GROUND SURFAC
PROJECTED 200 FT ± INTO BOR

RESISTIVITY CONTACT PROJECTED INTO SECTION
PARALLEL TO MAPPED CONTACT

CENTER OF SOUNDING

RESISTIVITY CONTACT PROJECTED INTO
SECTION PARALLEL TO MAPPED CONTACT

CE

10-C

8-C

$\rho' = 19$

$\rho = 123$

$\rho = 53$ ohm-ft

$\rho = 2C$ ohm-ft

CLAY PLUG CONTACT BY
RESISTIVITY PROFILE

CLAY PLUG CONTACT
BY RESISTIVITY
PROFILE

CLAY PLUG

$\rho = 114$ ohm-f

CLAY PLUG CONTACT
INFERRED FROM BORINGS

SCALE

0          500 FT

Fig

Figure 8. Geologic cross section in vicinity of geophysical traverses, Old River site (from References 10, 11, and 12)

DIRECTION OF TRAVERSE

GROUND SURFACE

$d$

$a$  $a$  $a$

₵ FIRST MEASUREMENT

₵ SECOND MEASUREMENT
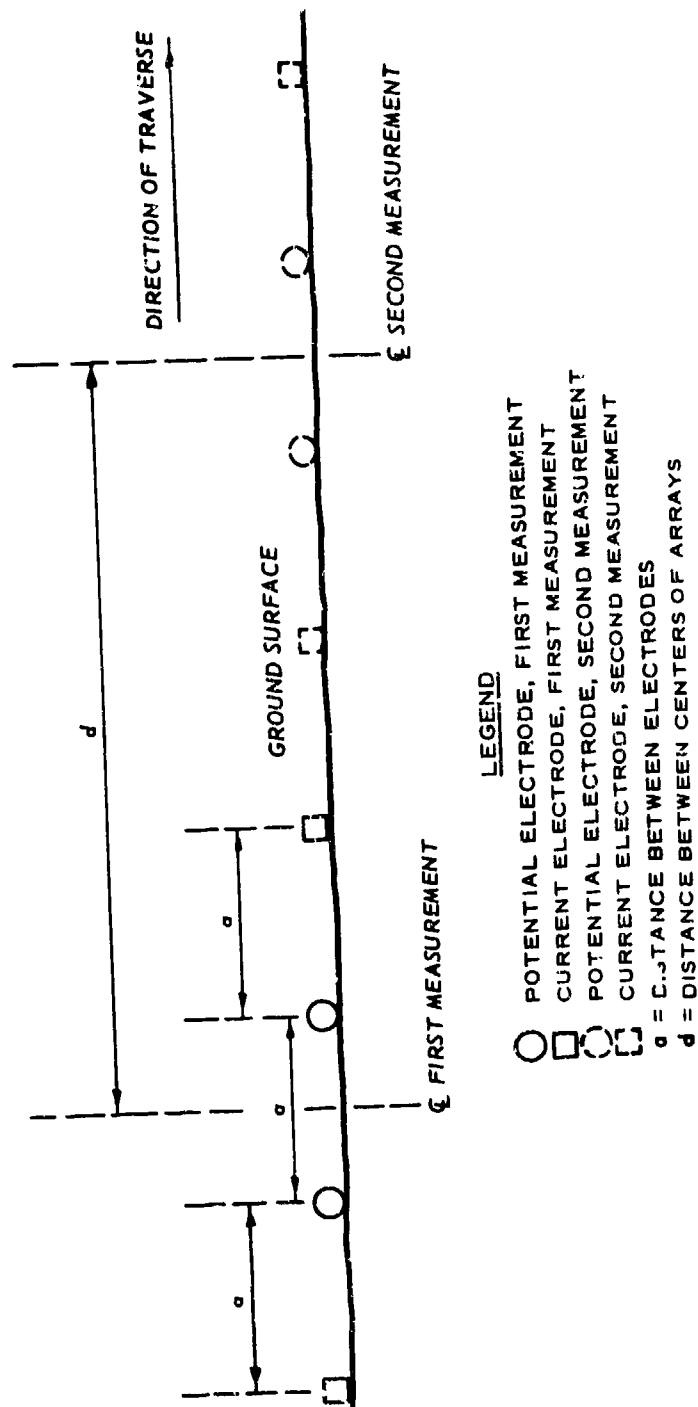
LEGEND

○ POTENTIAL ELECTRODE, FIRST MEASUREMENT
□ CURRENT ELECTRODE, FIRST MEASUREMENT
◌ POTENTIAL ELECTRODE, SECOND MEASUREMENT
⊡ CURRENT ELECTRODE, SECOND MEASUREMENT
$a$ = DISTANCE BETWEEN ELECTRODES
$d$ = DISTANCE BETWEEN CENTERS OF ARRAYS

Figure 9.  Configuration of typical Wenner array
resistivity profile. For a given profile,
"a" and "d" are constant. Resistivity
meter and cable reels not shown
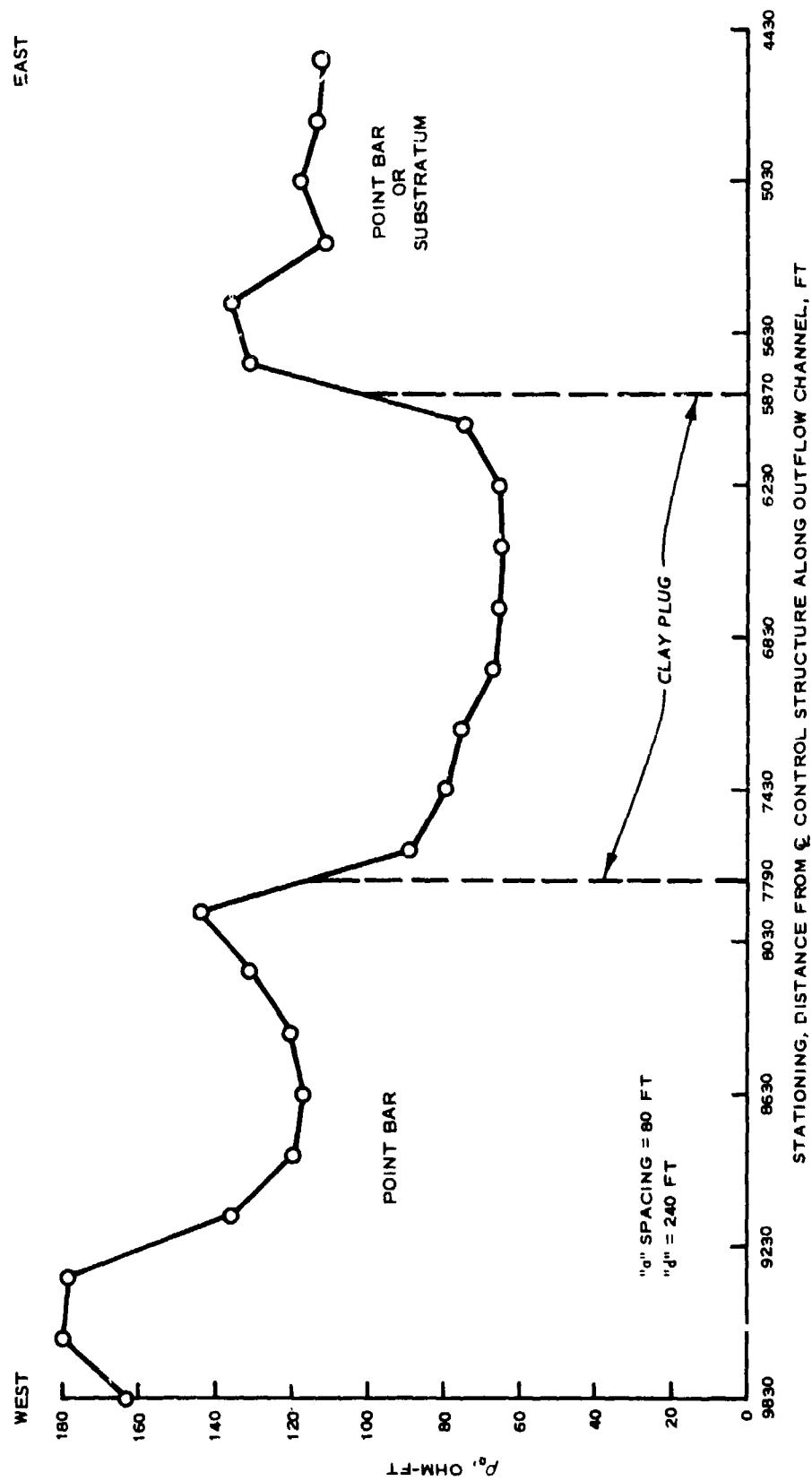
Figure 10. Graph of resistivity profile, Old River outflow channel
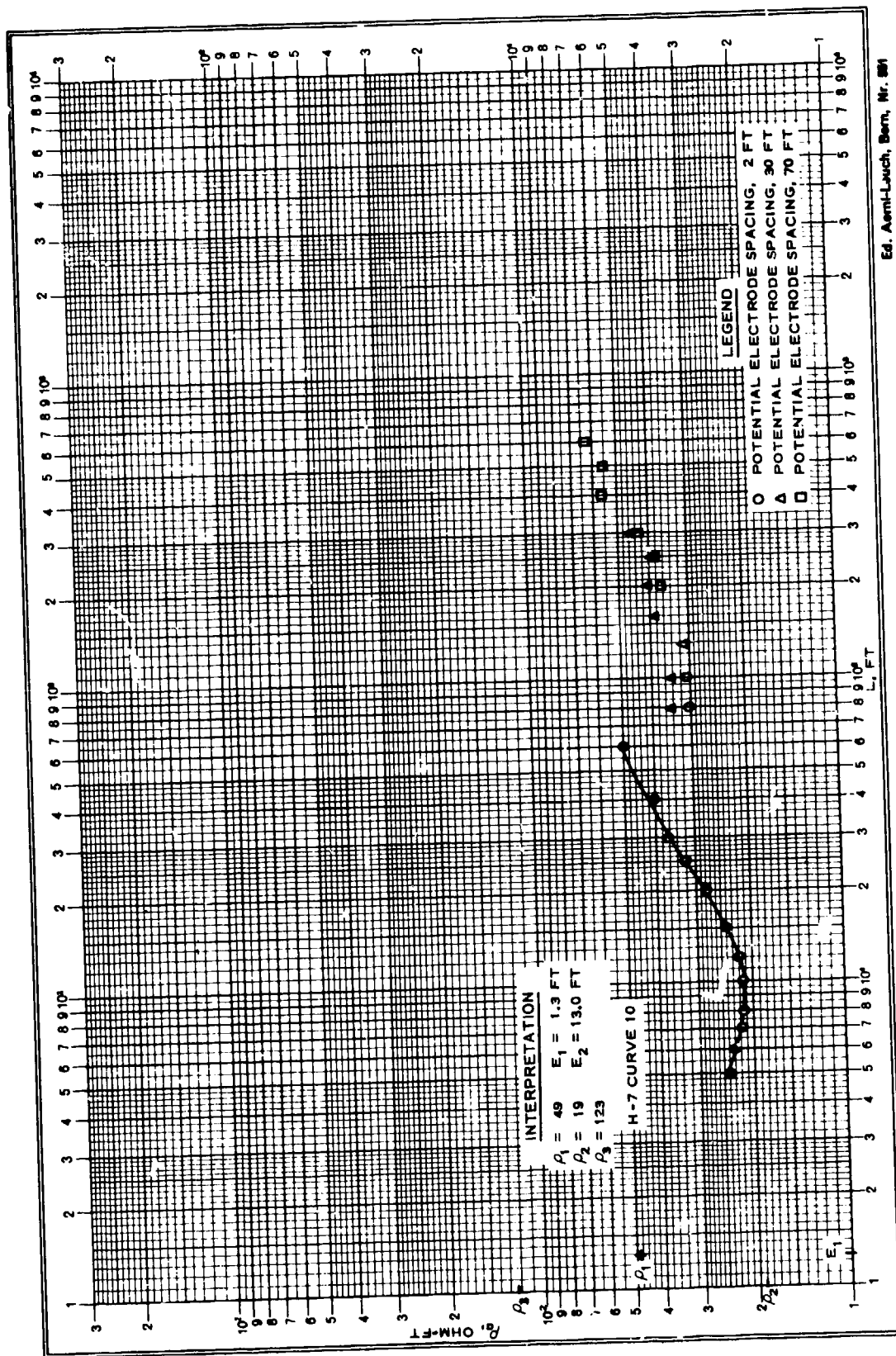
Figure 11. Field curve and interpretation, resistivity sounding in clay plug, Old River outflow channel
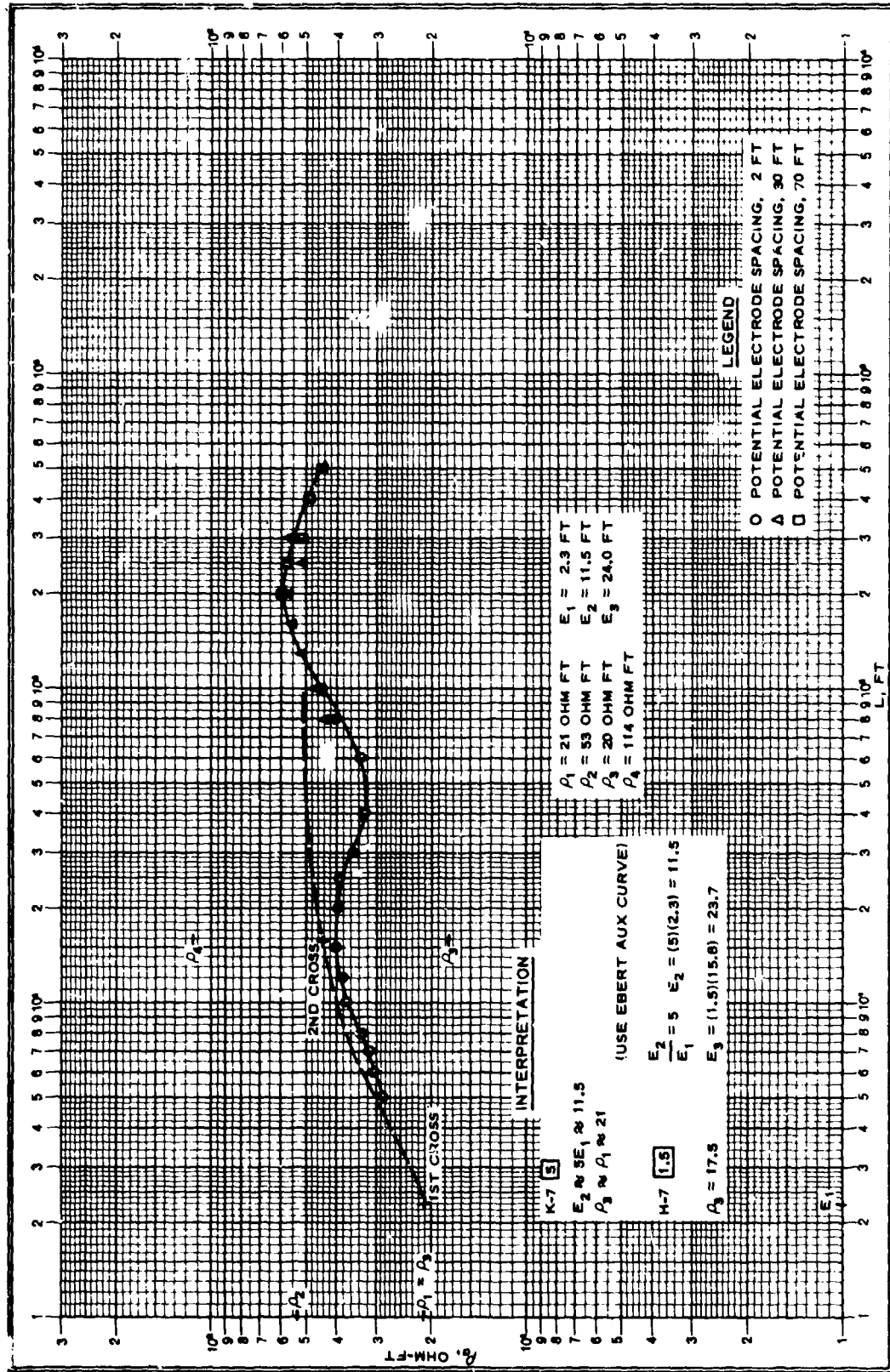
Figure 12. Field curve and interpretation, resistivity
sounding, east of clay plug, Old River outflow
channel

$$V_1 = \frac{X_2 - X_1}{T_2 - T_1} = \frac{5}{0.0155} = 323 \text{ FT/SEC}$$

$$V_2 = \frac{10 - 3}{0.0218 - 0.0165} = 943 \text{ FT/SEC}$$

$$V_3 = \frac{40 - 20}{0.0322 - 0.0272} = 4000 \text{ FT/SEC}$$

$$V_4' = \frac{70 - 50}{0.0614 - 0.044} = 1149 \text{ FT/SEC}$$

$$X_{c_1} = \sqrt{\frac{V_2 - V_1}{V_2 + V_1}} = 5.5\sqrt{\frac{943 - 323}{943 + 323}} = 1.9 \approx 2 \text{ FT}$$

$$D_1 = \frac{V_3 T'_3}{2} \times \frac{1}{\sqrt{\left(\frac{V_3}{V_1}\right)^2 - 1}} - D_1 \left[ \frac{\sqrt{\left(\frac{V_3}{V_1}\right)^2 - 1}}{\sqrt{\left(\frac{V_3}{V_2}\right)^2 - 1}} \right]$$

$$D_2 = \frac{4000 \times 0.022}{2} \times \frac{1}{\sqrt{\left(\frac{4000}{943}\right)^2 - 1}} - 1.9 \left[ \frac{\sqrt{\left(\frac{4000}{323}\right)^2 - 1}}{\sqrt{\left(\frac{4000}{943}\right)^2 - 1}} \right] = 10.7 \text{ FT} \approx 11 \text{ FT}$$

TIME, MSEC

DISTANCE, FT
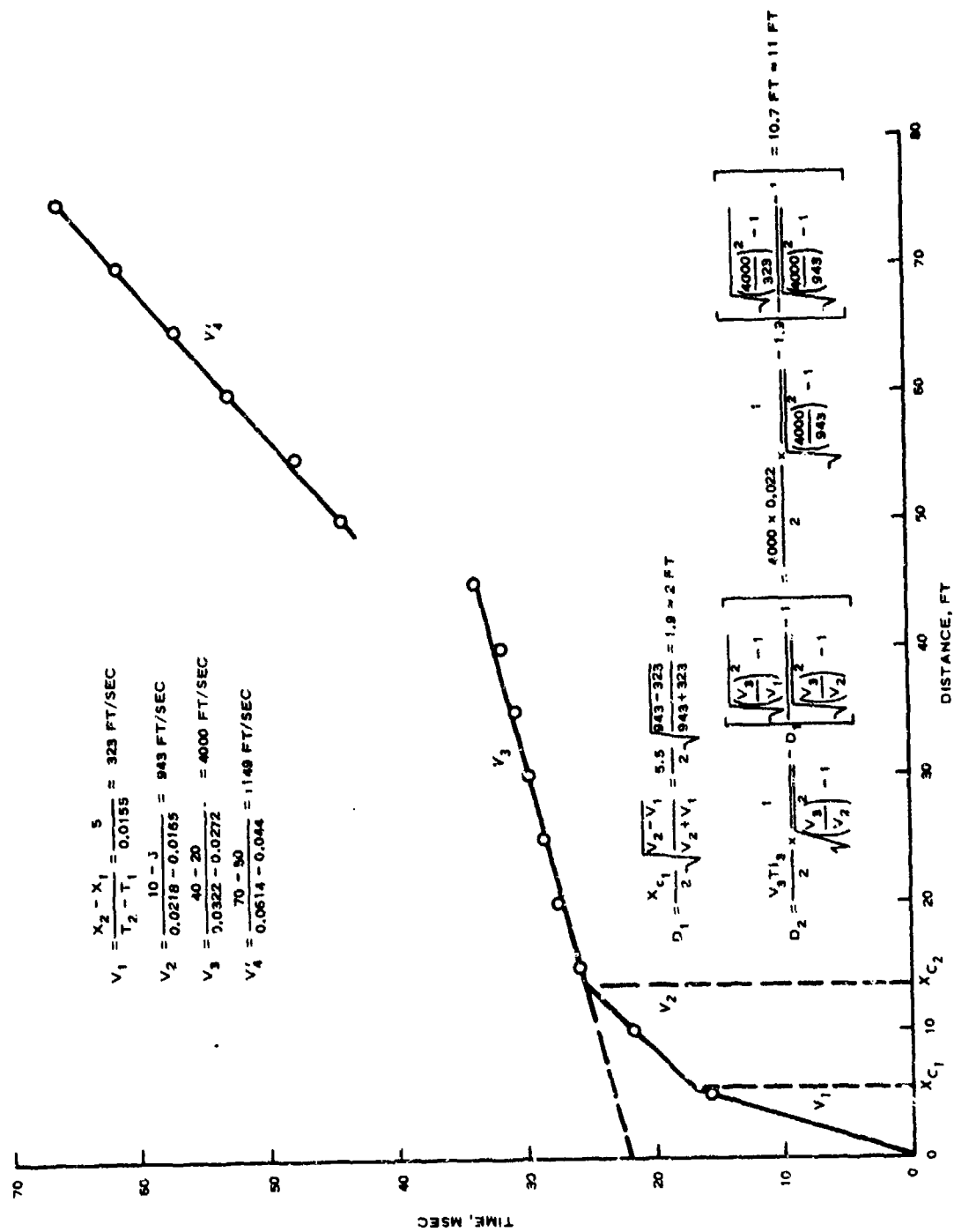
Figure 13. Field curve and interpretation, seismic refraction line, Sta 1 (clay plug), Old River outflow channel
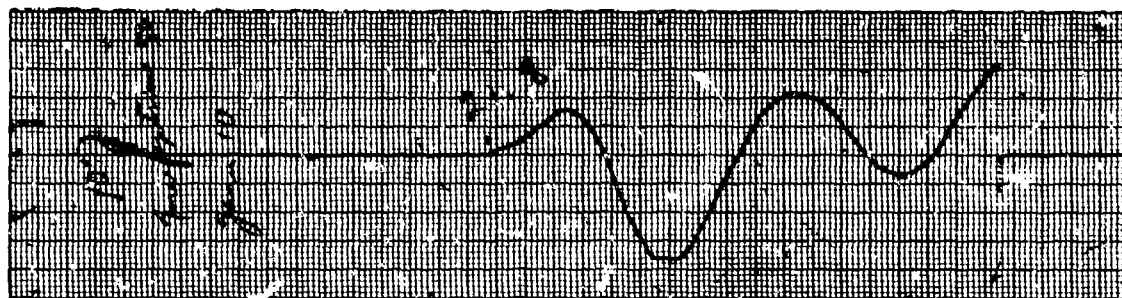
a. HAMMER STATION 10 FT FROM GEOPHONE, TRAVEL TIME = 21.8 MSEC
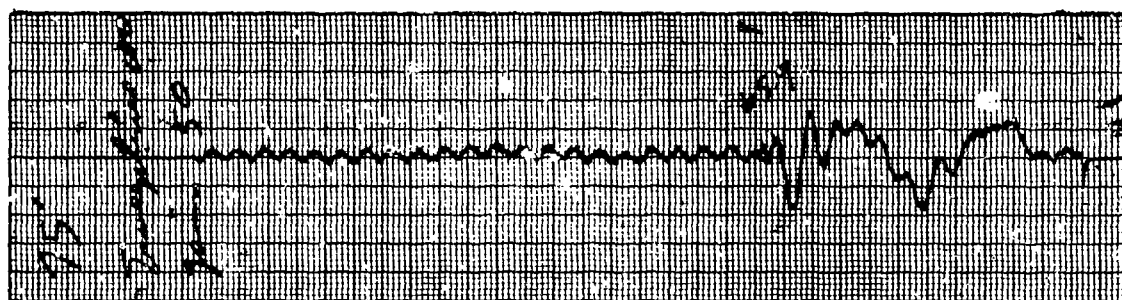


b. HAMMER STATION 75 FT FROM GEOPHONE, TRAVEL TIME = 65.9 MSEC
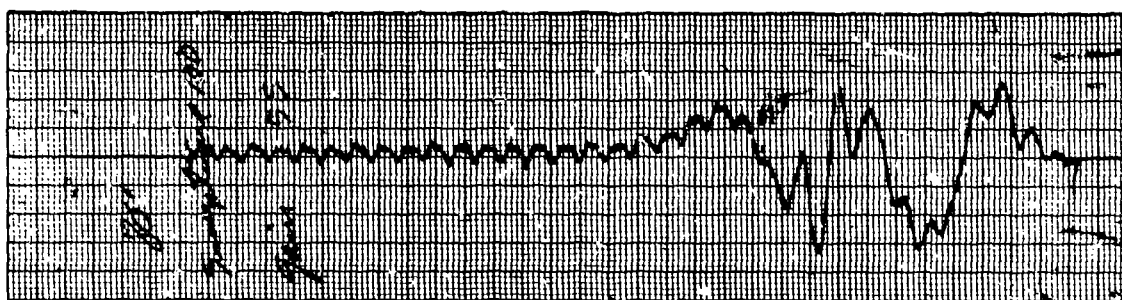


c. HAMMER STATION 80 FT FROM GEOPHONE, TRAVEL TIME DIFFICULT
TO DETERMINE

Figure 14. Strip-chart records for compression wave arrivals at three hammer stations, clay plug seismic line, Old River outflow channel. Signal quality degenerates from a. to c.
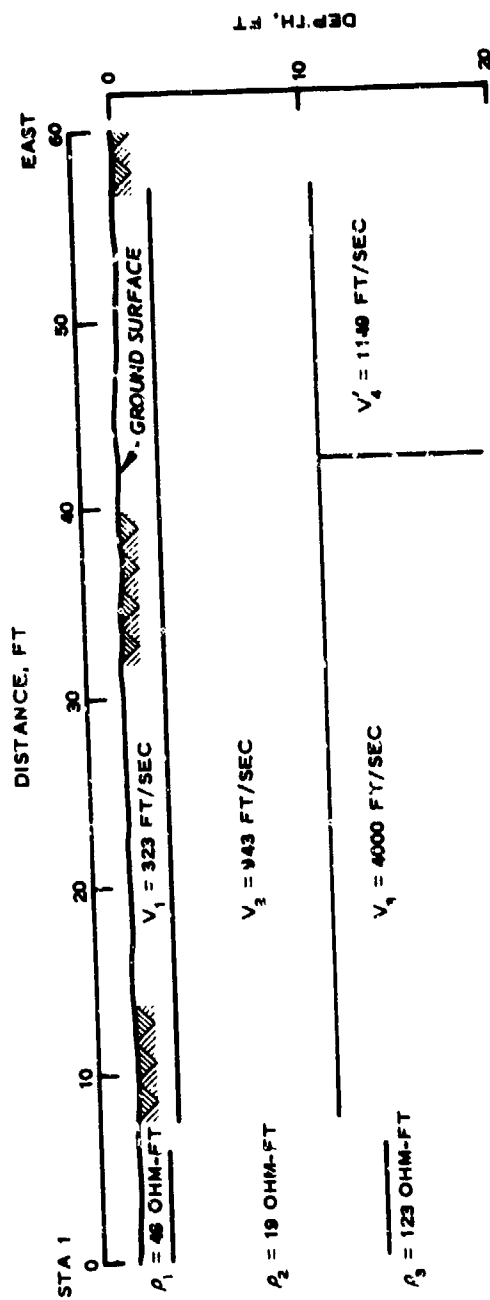
Figure 15. Simplified geologic section for sta 1, Old River outflow channel, based on seismic data, with resistivity section superposed

AN ALTERNATE, AND MORE LIKELY, INTERPRETATION IS THAT THE 1128 FT/SEC LAYER IS UNDERLAIN BY A THICK LOWER VELOCITY LAYER THAT PRECLUDES THE ARRIVAL OF THE REFRACTED WAVE

INTERPRETATION

$V = \dfrac{300}{0.266} = 1128$ FT/SEC

MINIMUM DEPTH TO HIGH VELOCITY LAYER $= D_{min}$

$D_{min} = \dfrac{X_{max}}{2} \sqrt{\dfrac{V_2 - V_1}{V_2 + V_1}}$ , WHERE $X_{max} = 300$ FT

$V_1 = 1128$ FT/SEC

$V_2$ ESTIMATED AT 4500 FT/SEC (SATURATED SAND)

$= \dfrac{300}{2} \sqrt{\dfrac{4500 - 1128}{4500 + 1128}}$

$= 115$ FT

TIME, MSEC

DISTANCE, FT

EAST

WEST

Figure 16. Seismic refraction data, sta 2, Old River outflow channel, line running east to west
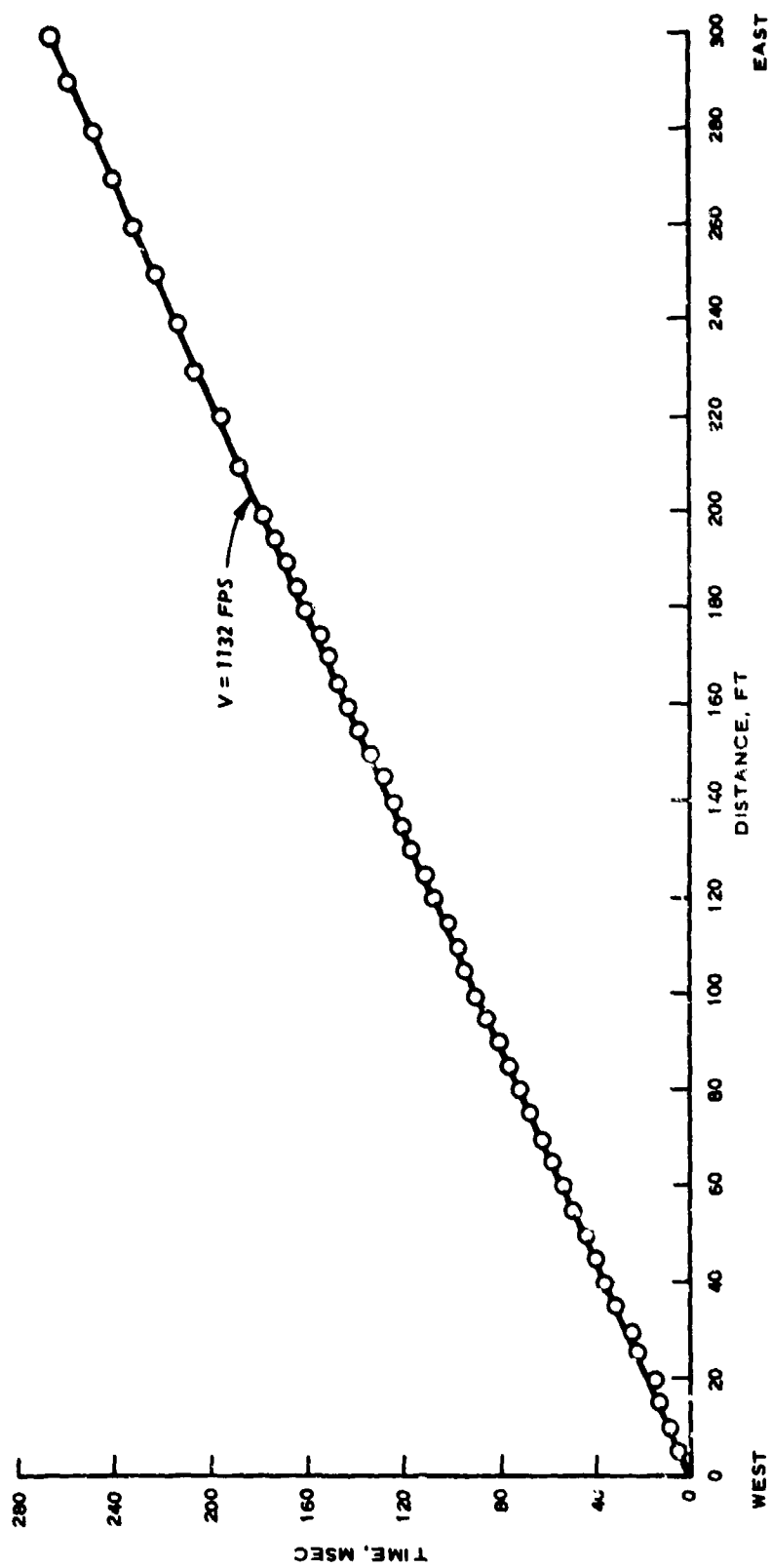
Figure 17. Seismic refraction data, sta 2, Old River outflow channel, line running west to east
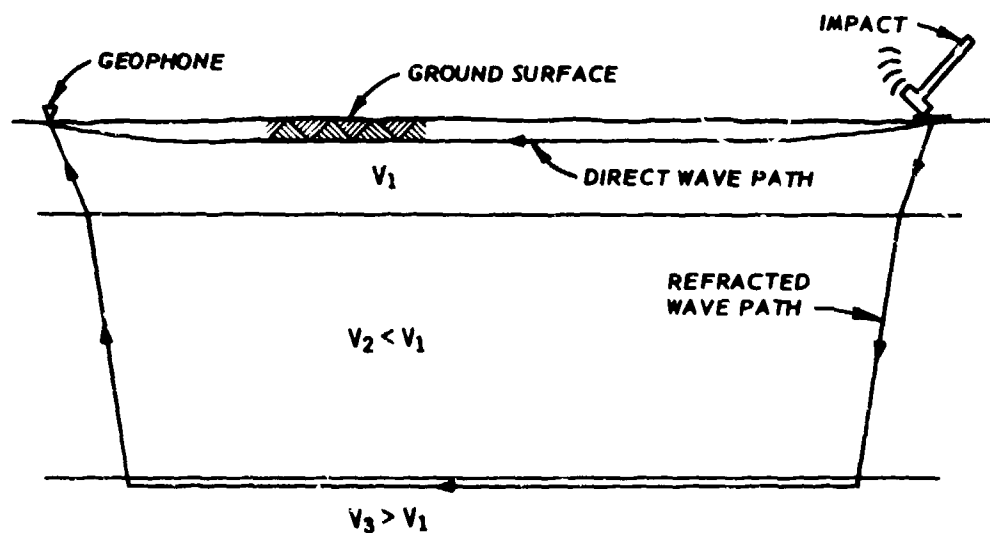
Figure 18. Hypothetical cross section to explain time-
distance curves produced by seismic refraction
line at sta 2, Old River outflow channel
(Figures 16 and 17). Direct wave arrives before
refracted wave at every impact point
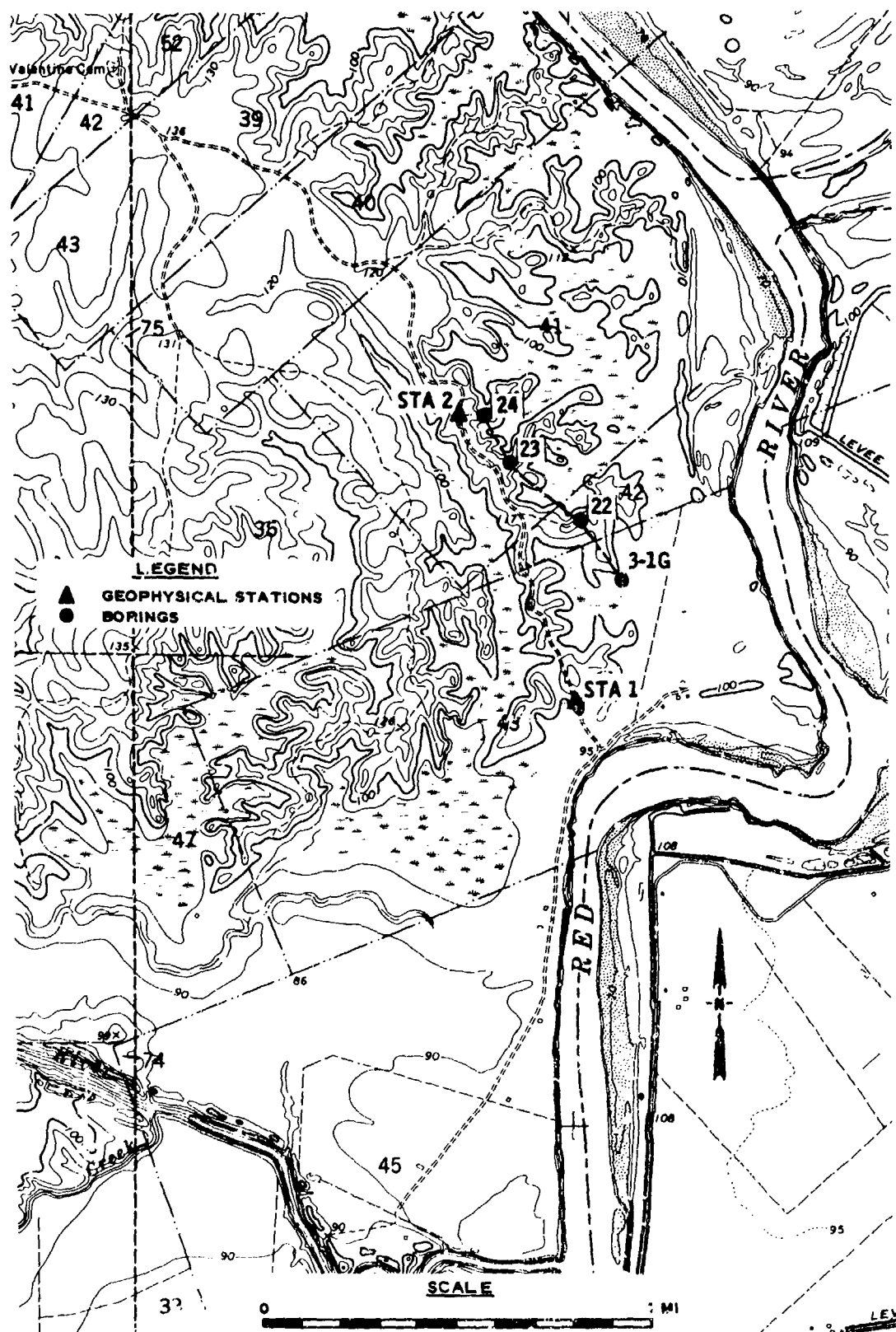
Figure 19.   Map of Lock and Dam No. 3, Red
River, site (Boyce 7-1/2 min quad)

STUDY AREA

RED RIVER

SCALE

| 1 | 0.5 | 0 | 1 | 2 MI |

N

LEGEND

QUATERNARY

RECENT

NATURAL LEVEE

POINT BAR

BACKSWAMP

ABANDONED CHANNEL

ABANDONED COURSE

UNDIFFERENTIATED ALLUVIUM OF SMALL CREEKS

PLEISTOCENE

MONTGOMERY TERRACE

TERTIARY

MIOCENE

FLEMING FORMATION

CATAHOULA FORMATION

ELEVATION OF TOP OF TERTIARY DEPOSITS IN FEET MSL
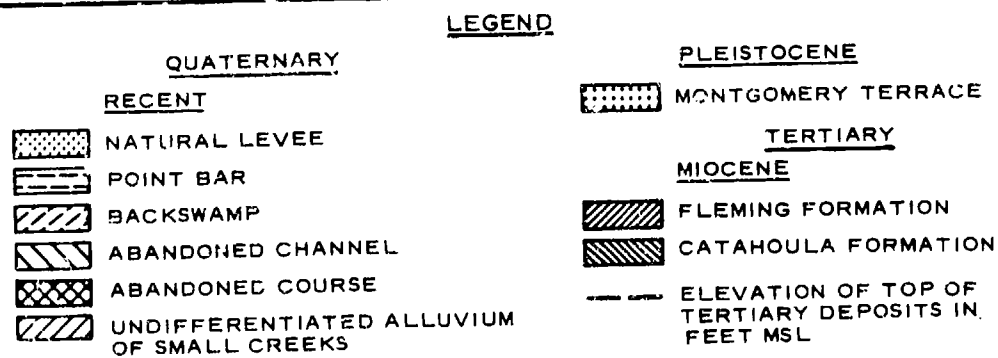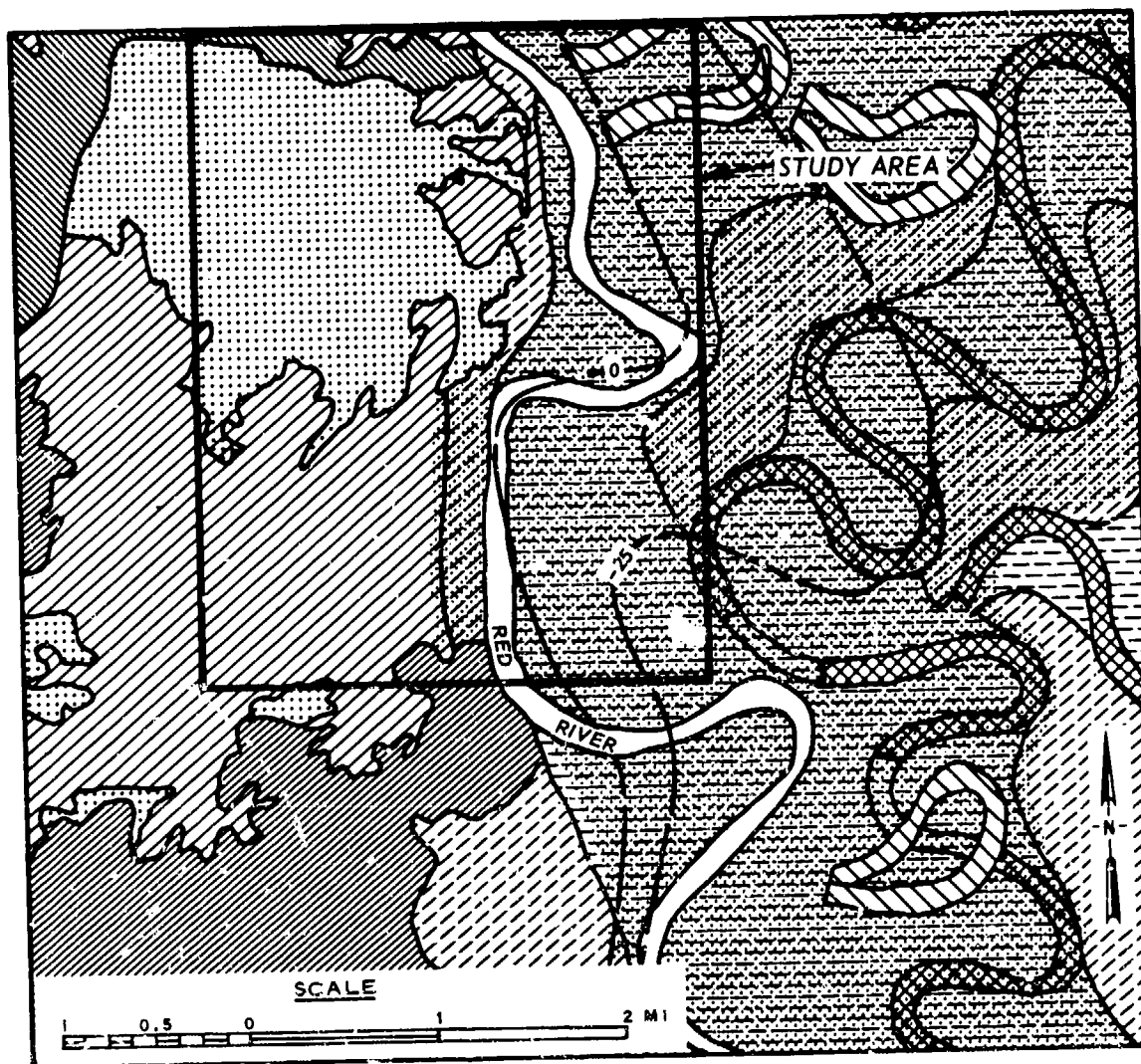
Figure 20.   Geologic map, Lock and Dam No. 3 site
(Boyce 15 min quad)

Figure 21. Boring logs, Lock and Dam No. 3 site (see map, Figure 19). Resistivity sounding data shown for correlation
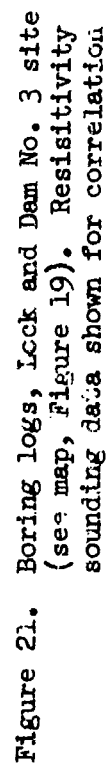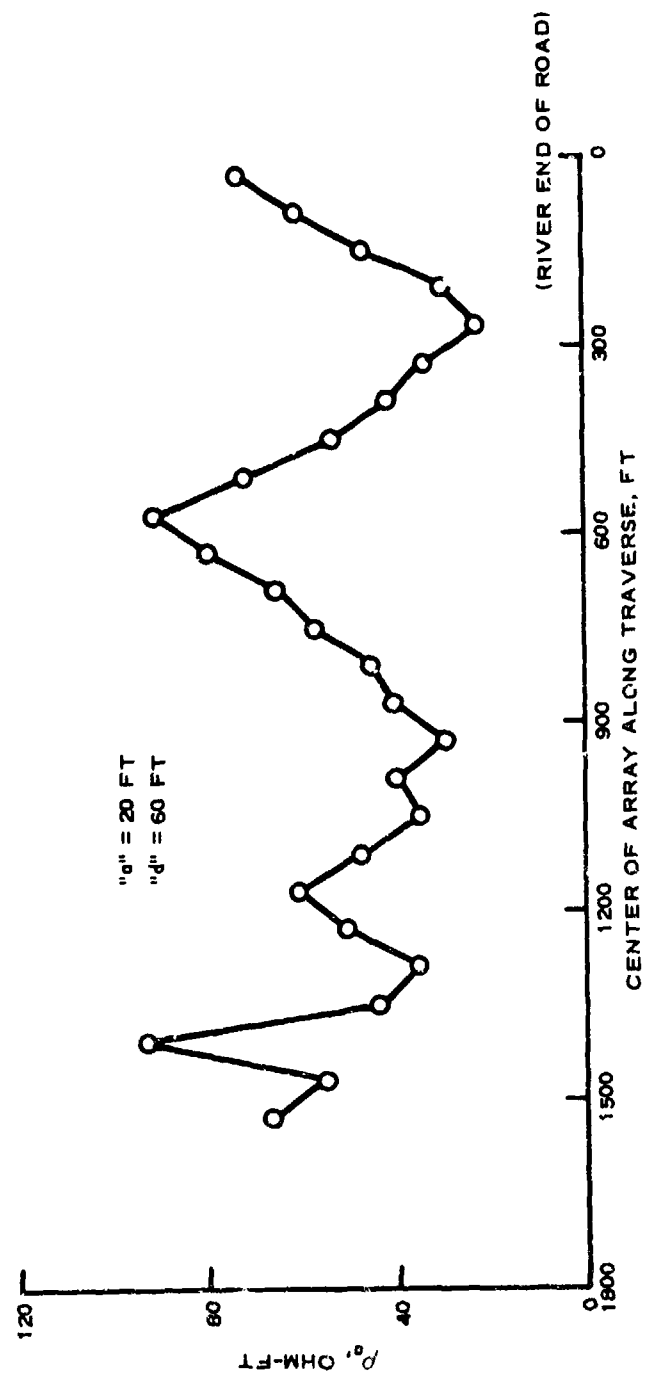
Figure 22. Resistivity profile graph for traverse along road, Lock and Dam No. 3 site, Red River
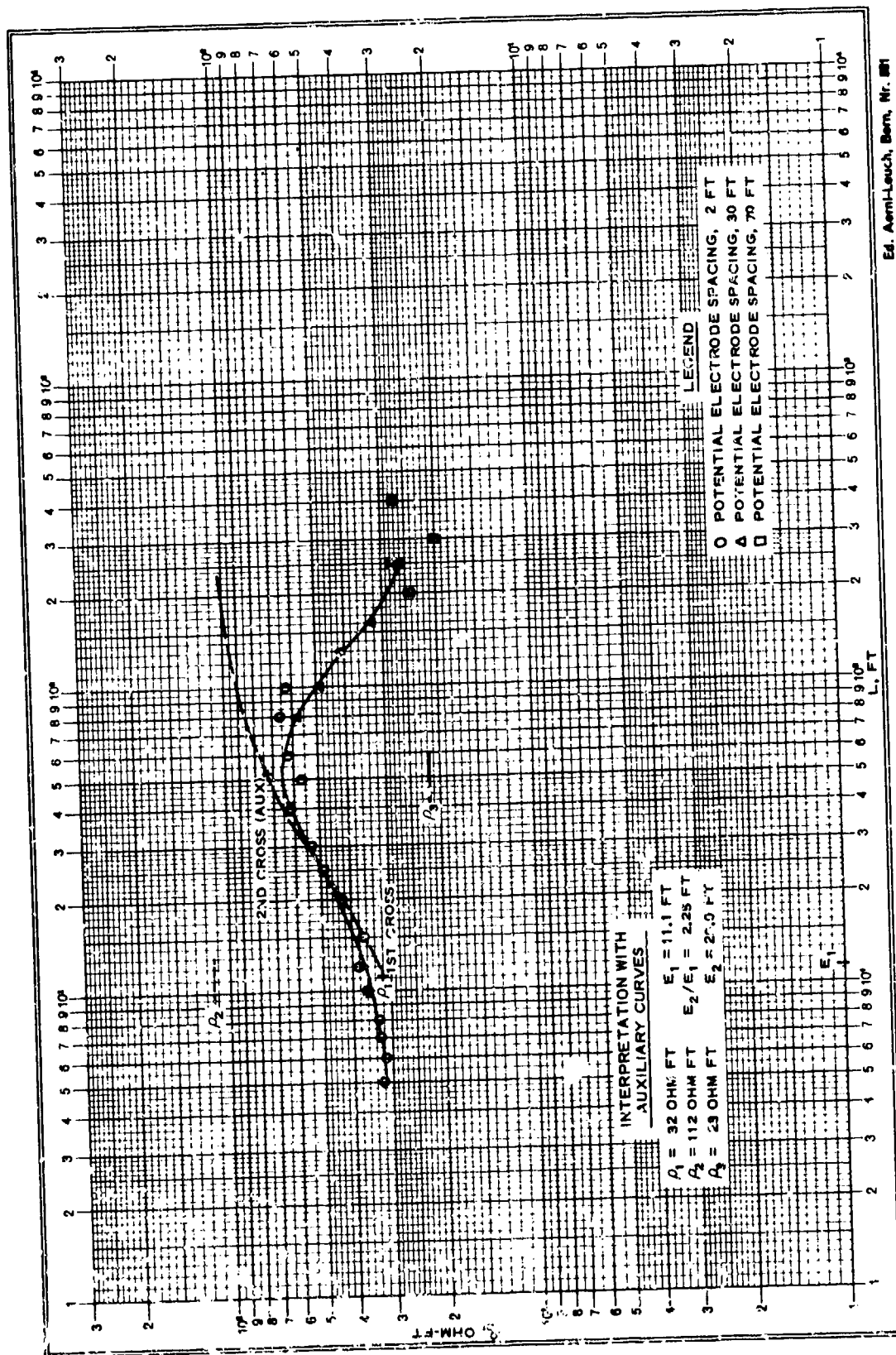
Figure 23. Field curve and interpretation, resistivity sounding, sta 1, Lock and Dam No. 3 site, Red River
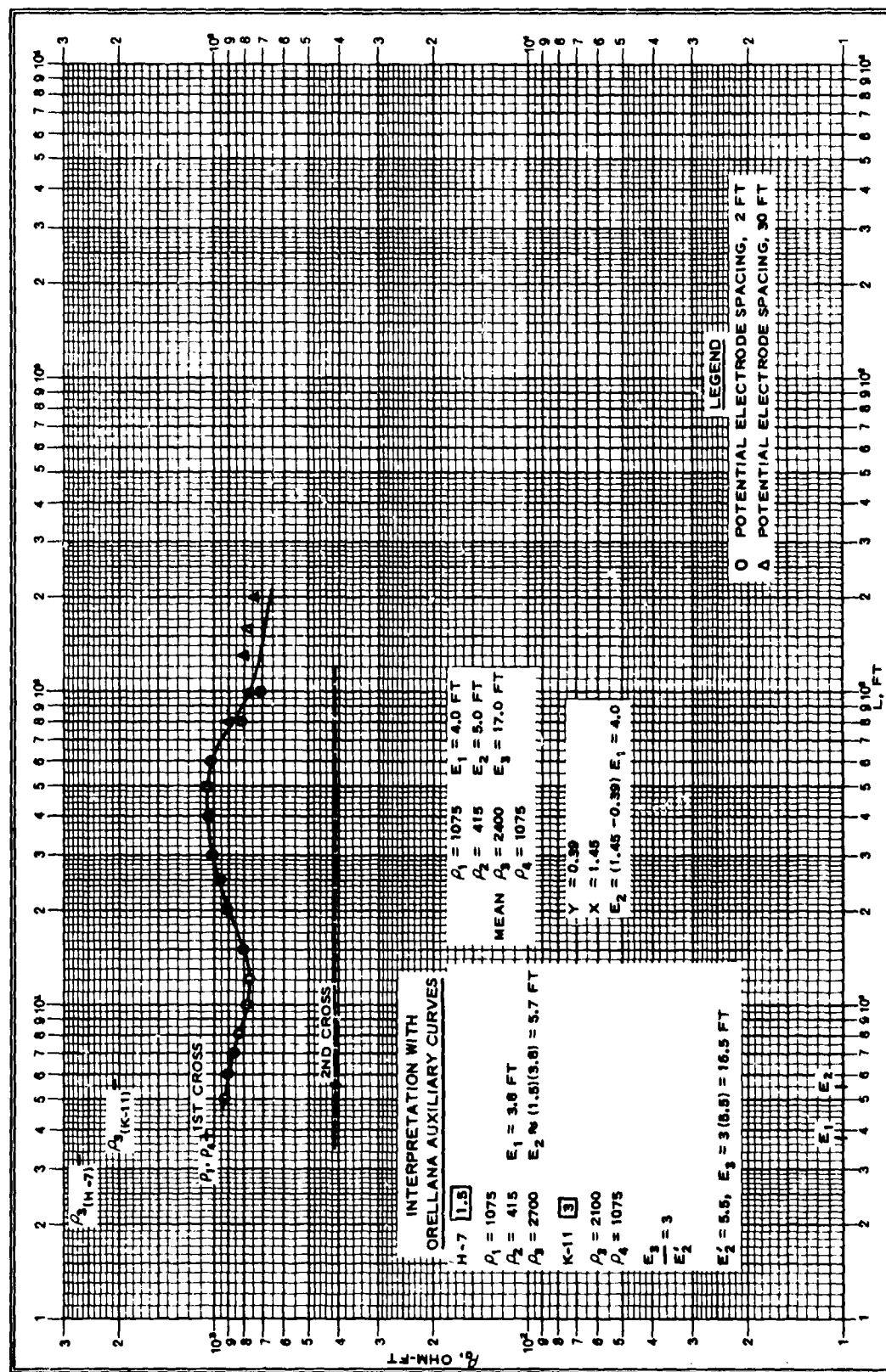
Figure 24. Field curve and interpretation, resistivity
sounding, sta 2, Lock and Dam No. 3 site, Red River

$V_1 = \dfrac{21}{0.020} = 1050 \text{ FT/SEC}$

$V_{2A} = \dfrac{260 - 100}{0.066 - 0.0371} = 5536 \text{ FT/SEC}$

$V_{2B} = \dfrac{260 - 100}{0.066 - 0.0357} = 5281 \text{ FT/SEC}$

NEGLIGIBLE ELEVATION DIFFERENCE IN GROUND SURFACE

$\theta = \frac{1}{2}\left[\sin^{-1}\dfrac{V_1}{V_{2B}} - \sin^{-1}\dfrac{V_1}{V_{2A}}\right] = \frac{1}{2}\left[\sin^{-1}\dfrac{1050}{5281} - \sin^{-1}\dfrac{1050}{5536}\right]$

$\theta = 0.27°$ (NEGLIGIBLE)

$V_2 = 2\cos\theta \times \dfrac{V_{2A} \times V_{2B}}{V_{2A} + V_{2B}} = 2\,\dfrac{5536 \times 5281}{5536 + 5281} = 5405 \text{ FT/SEC}$

$D_{1A} = \dfrac{V_1 T_{iA}}{2\cos\theta} \times \dfrac{1}{\sqrt{1 - \left(\frac{V_1}{V_2}\right)^2}} = \dfrac{1050 \times 0.0192}{\sqrt{1 - \left(\frac{1050}{5405}\right)^2}} = 10.3 \text{ FT}$

$D_{1B} = \dfrac{V_1 T_{iB}}{2\cos\theta} \times \dfrac{1}{\sqrt{1 - \left(\frac{V_1}{V_2}\right)^2}} = \dfrac{1050 \times 0.0168}{\sqrt{1 - \left(\frac{1050}{5405}\right)^2}} = 9.0 \text{ FT}$

CURVED SLOPE INDICATES UNIFORM INCREASE IN $V_1$ WITH DEPTH

Figure 25. Seismic refraction data, sta 1, west to east line, Lock and Dam No. 3 site, Red River

Figure 26. Seismic refraction data, sta 1, east to west line, Lock and Dam No. 3 site, Red River

INTERPRETATION

$V_1$ (EF and D) $= \dfrac{50}{0.030} = 1667$ FT/SEC

$V_{2A} = \dfrac{50}{0.0292} = 4762$ FT/SEC

$V_{2B} = \dfrac{230-55}{0.067-0.042} = 7000$ FT/SEC

GROUND SURFACE SLOPES AS A MONOCLINE, 10 FT HIGHER AT 230 FT (WEST) THAN AT 0 (EAST). REFER ALL DIPS AND DEPTHS TO THE SLOPING SURFACE.

$\theta$ (dip) $= \frac{1}{2}\left[\sin^{-1}\dfrac{V_1}{V_{2B}} - \sin^{-1}\dfrac{V_1}{V_{2A}}\right] = \frac{1}{2}\left[\sin^{-1}\dfrac{1667}{7000} - \sin^{-1}\dfrac{1667}{4762}\right] = -3.4°$

$V_2 = 2\cos\theta \dfrac{V_{2A} \times V_{2B}}{V_{2A}+V_{2B}} = 2\cos 3.4 \dfrac{4762 \times 7000}{4762 + 7000} = 5658$ FT/SEC

DEPTH AT A $= \dfrac{V_1 T_{iA}}{2\cos\theta} \times \dfrac{1}{\sqrt{1-\left(\frac{V_1}{V_2}\right)^2}} = \dfrac{1667 \times 0.0186}{2(0.996)} \times \dfrac{1}{\sqrt{1-\left(\frac{1667}{5658}\right)^2}}$

$D_A = 16.2$ FT

DEPTH AT B $(D_B) = \dfrac{V_1 T_{iB}}{2\cos\theta} \times \dfrac{1}{\sqrt{1-\left(\frac{V_1}{V_2}\right)^2}}$ WHERE $T_{iB} = 0.0342$ SEC

$-D_B = 29.8$ FT

ERRATIC POINTS IN LOWER LAYER MAY INDICATE PRESENCE OF TERTIARY BEDROCK BOULDERS ENTRAINED IN TERRACE MATERIAL

$V_{2B} = 7000$ FT/SEC

$V_{2A} = 4762$ FT/SEC

$V_1 = 1667$ FT/SEC

$V_1 = 1667$ FT/SEC

DISTANCE, FT

TIME, MSEC

EAST A

WEST B

Figure 27. Section based on seismic data, sta 1, Lock and Dam No. 3 site, Red River, along line of traverses (road)
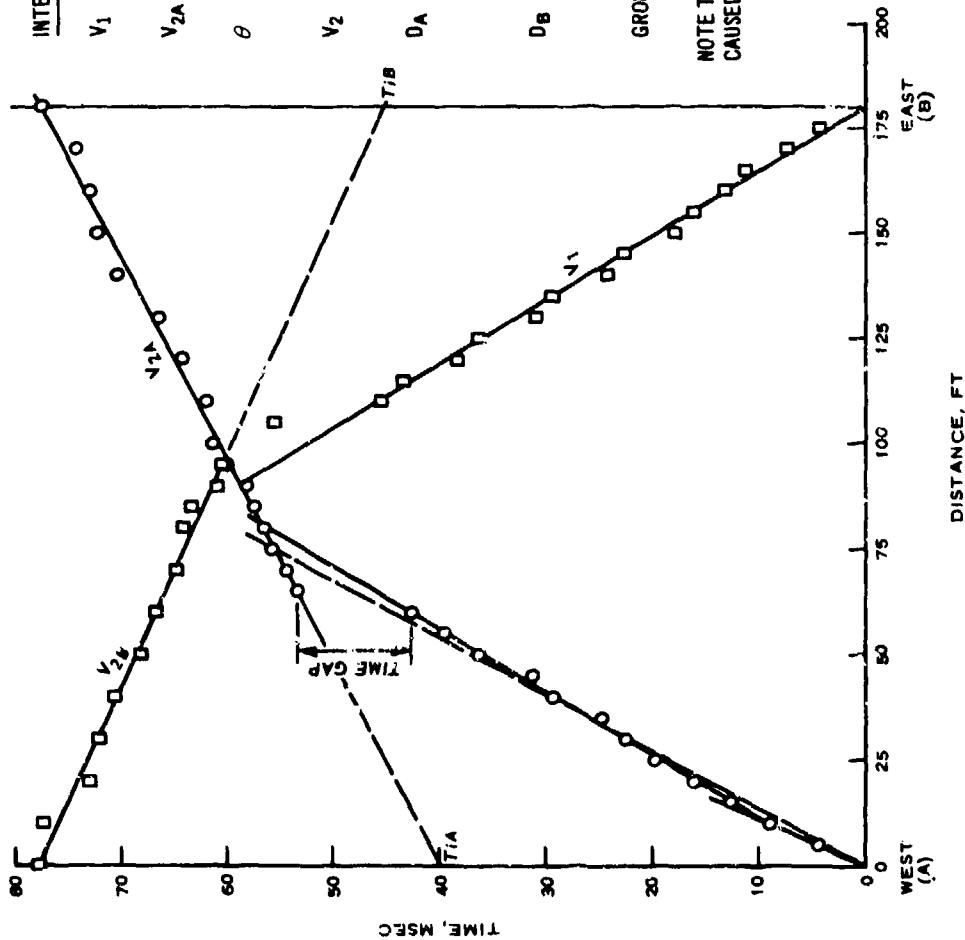
$V_1 = \dfrac{76}{0.050} = 1520$ FT/SEC

$V_{2A} = \dfrac{180-0}{0.0776-0.0398} = 4762$ FT/SEC $\quad V_{2B} = \dfrac{180-0}{0.0776-0.0452} = 5556$ FT/SEC

$\theta = \frac{1}{2}\left[\sin^{-1}\dfrac{V_1}{V_{2B}} - \sin^{-1}\dfrac{V_1}{V_{2A}}\right] = \frac{1}{2}\left[\sin^{-1}\dfrac{1520}{5556} - \sin^{-1}\dfrac{1520}{4762}\right] = -1.4^\circ$

$V_2 = 2\cos\theta\ \dfrac{V_{2A}\times V_{2B}}{V_{2A}+V_{2B}} = 2\cos 1.4\ \dfrac{4762\times 5556}{4762+5556} = 5127$ FT/SEC

$D_A = \dfrac{V_1 T_{iA}}{2\cos\theta}\times\dfrac{1}{\sqrt{1-\left(\frac{V_1}{V_2}\right)^2}} = \dfrac{1520\times 0.0399}{2}\times\dfrac{1}{\sqrt{1-\left(\frac{1520}{5127}\right)^2}} = 31.8$ FT

$D_B = \dfrac{V_1 T_{iB}}{2\cos\theta}\times\dfrac{1}{\sqrt{1-\left(\frac{V_1}{V_2}\right)^2}} = \dfrac{1520\times 0.0453}{2}\times\dfrac{1}{\sqrt{1-\left(\frac{1520}{5127}\right)^2}} = 36.0$ FT

GROUND SURFACE RISES 8 FT FROM A TO B.

NOTE TIME GAP FROM $V_1$ TO $V_2$, BOTH FORWARD AND REVERSE. THIS MAY BE CAUSED BY A THIN LOW VELOCITY LAYER AT THE BASE OF LAYER $V_1$.



Figure 28. Seismic refraction data, sta 2, Lock and Dam No. 3 site, Red River
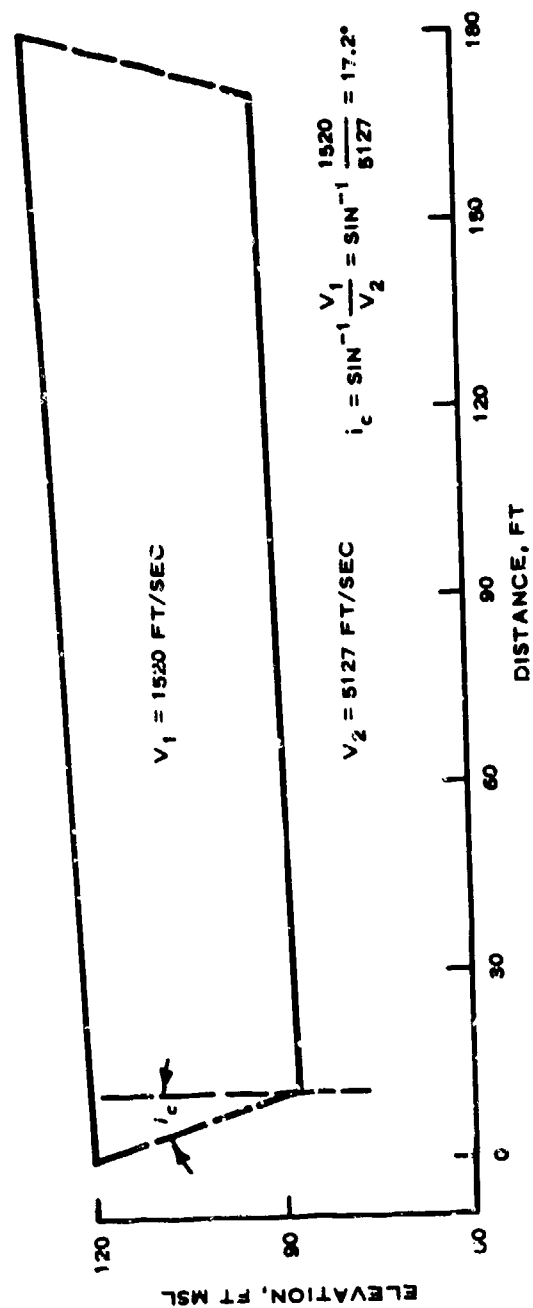
Figure 29. Inferred cross section based on seismic data, sta 2, Lock and Dam No. 3 site, Red River
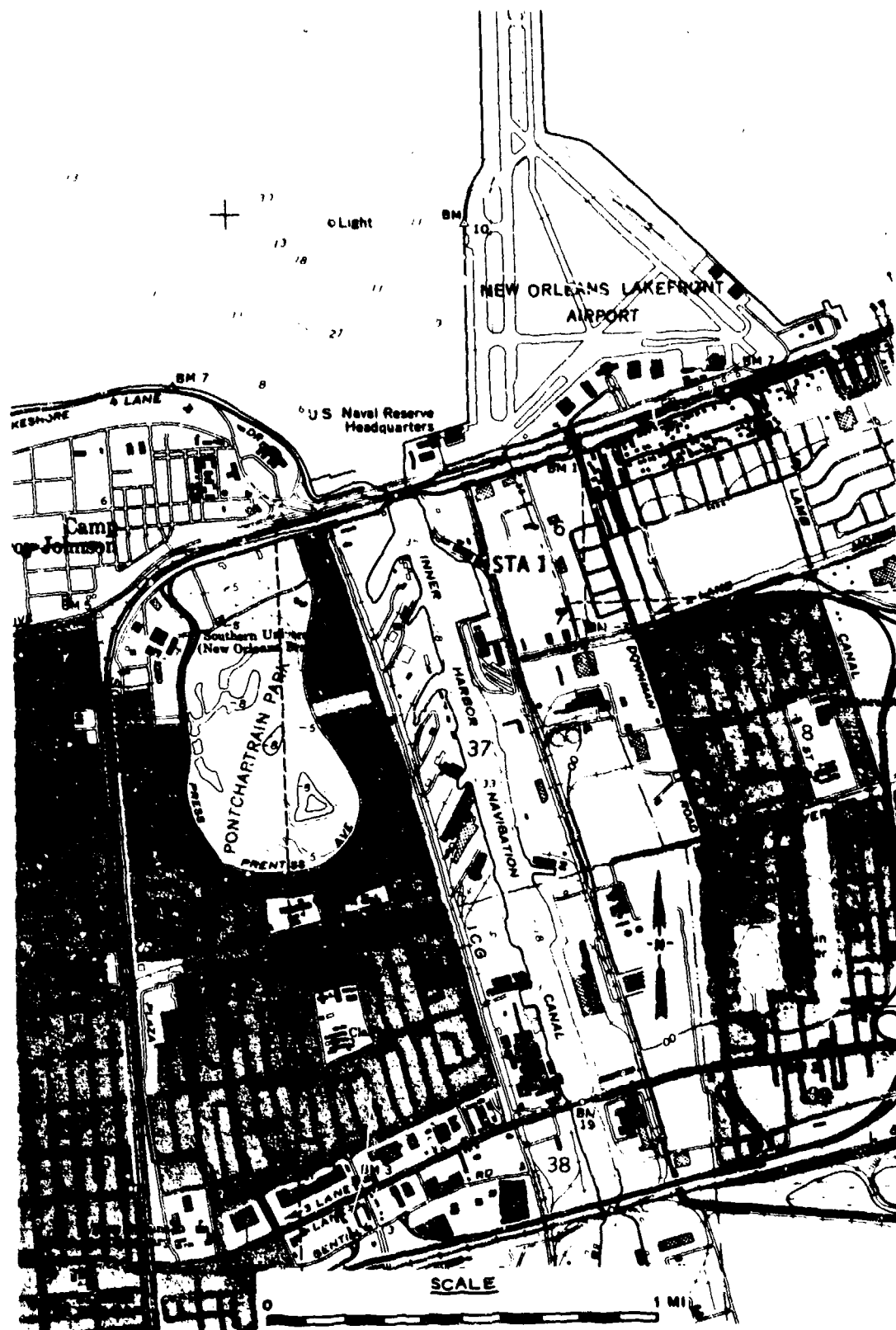
Figure 30.  Map of Inner Harbor Navigation Canal site,
New Orleans, La. (from Spanish Fort 7-1/2
min quad)
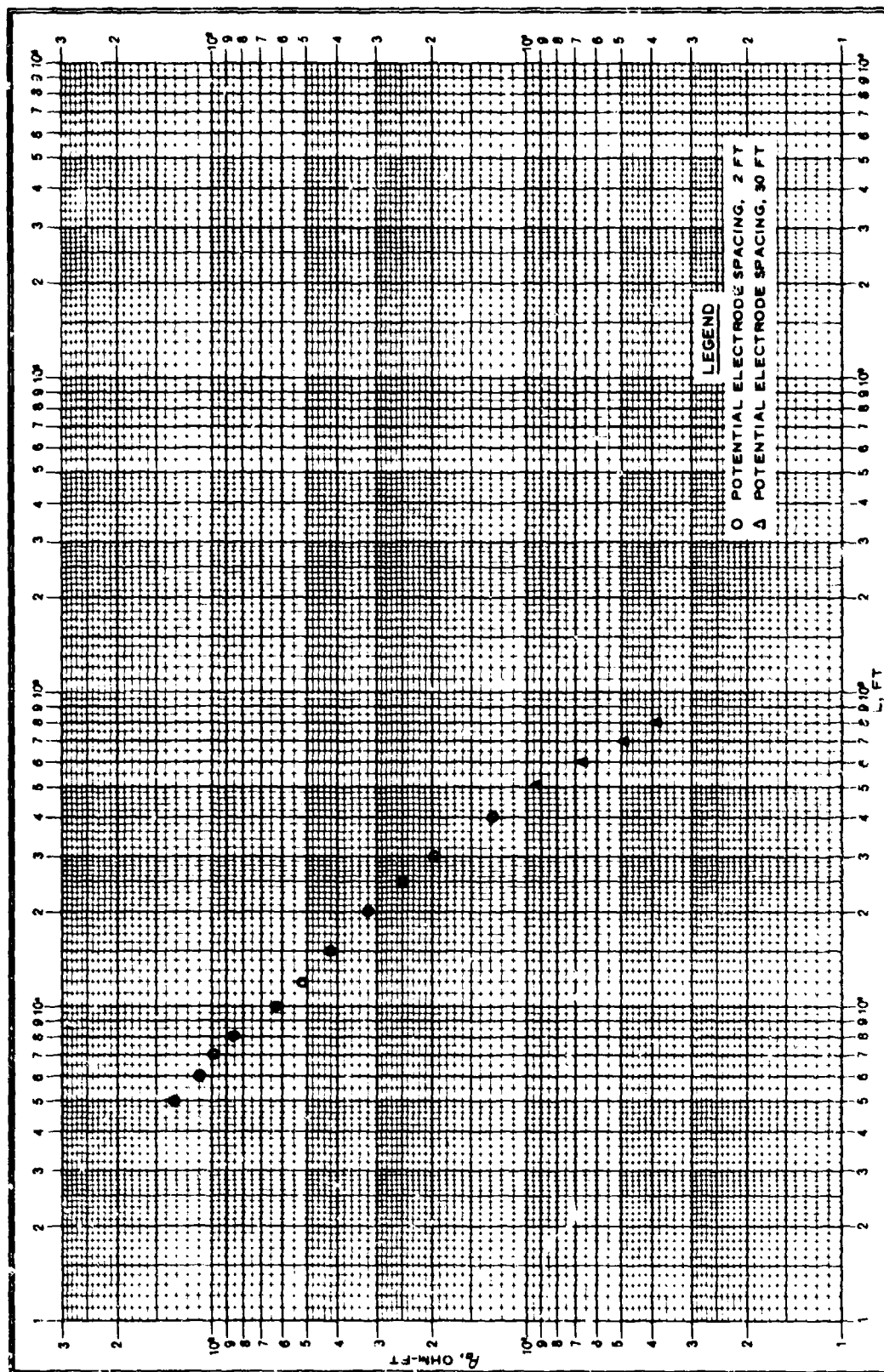
Figure 31.  Field curve, resistivity sounding,
Inner Harbor Navigational Canal site,
New Orleans
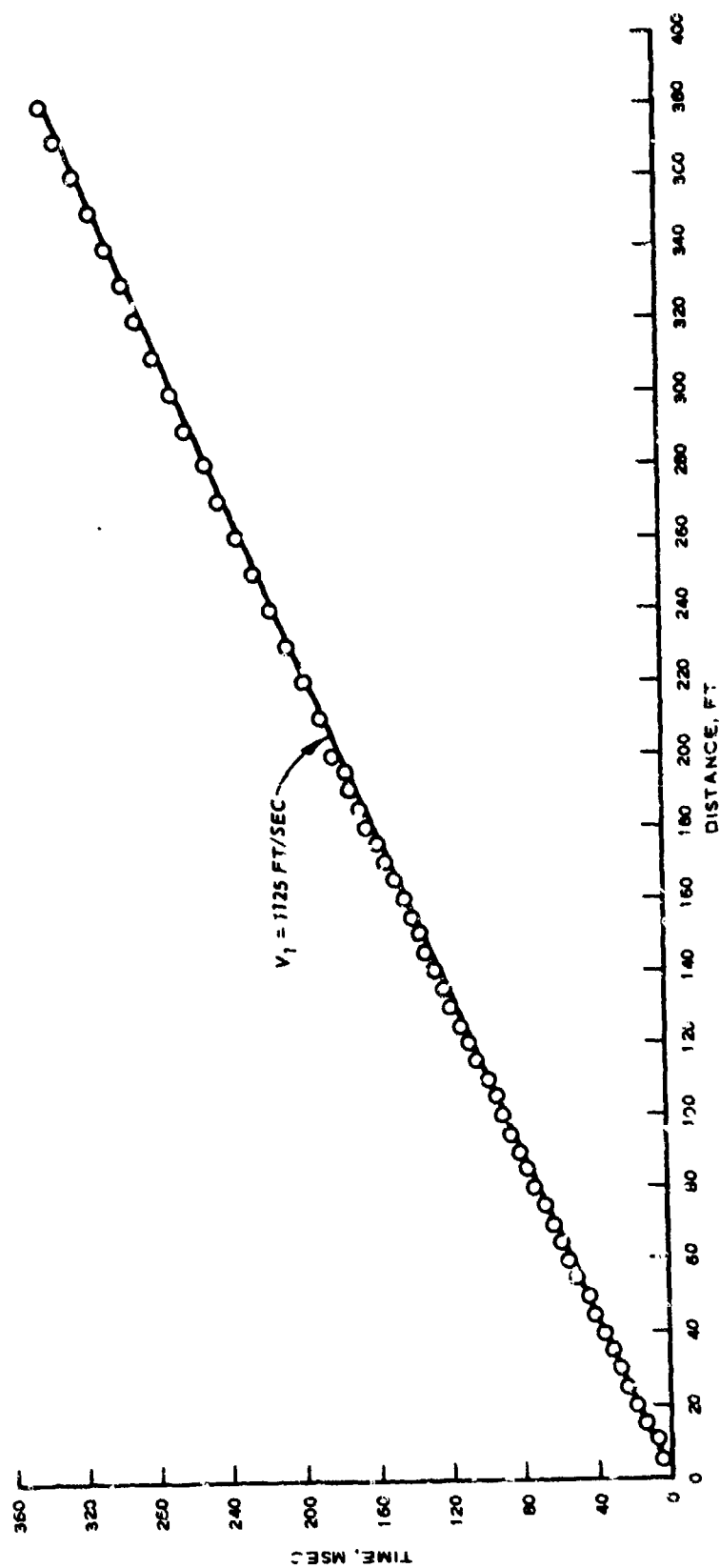
Figure 32. Seismic refraction data, Inner Harbor
Navigational Canal site, New Orleans
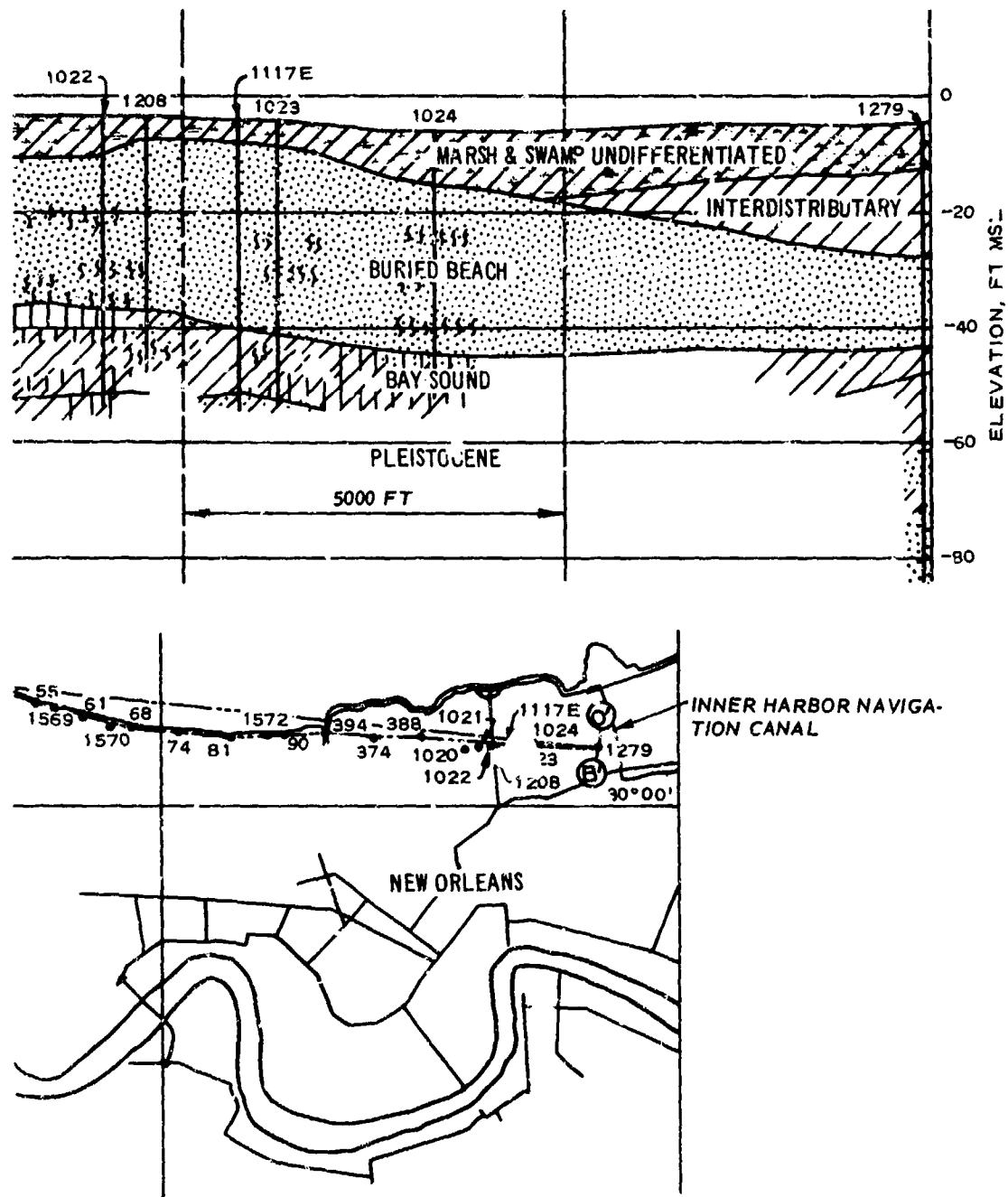
Figure 33. Geologic section (map inset) near Inner Harbor
Navigation Canal, New Orleans, showing marsh
and swamp deposits and interdistributary clays
overlying buried beach sands (from Reference 13)
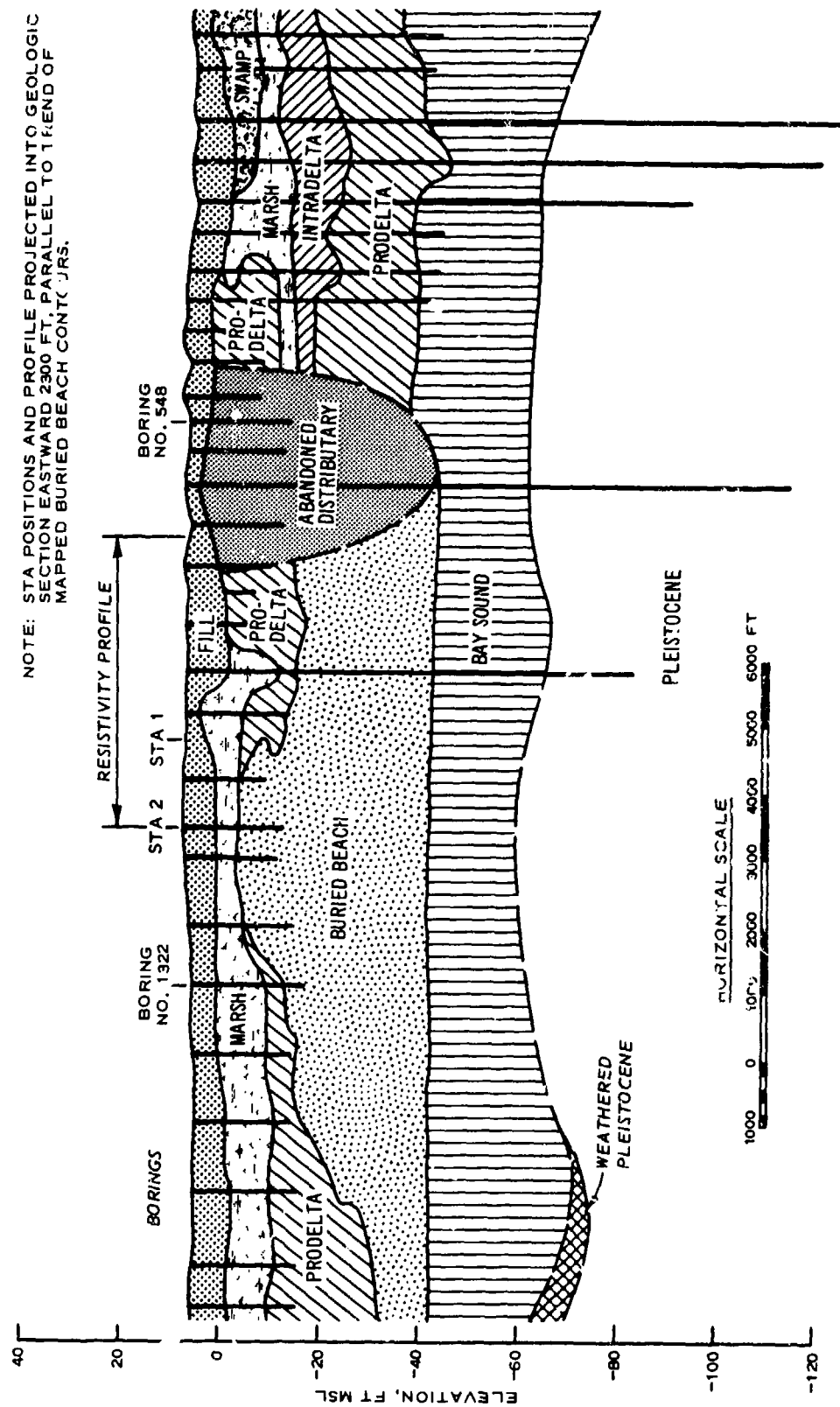
Figure 34. Geologic section in vicinity of Metairie Outfall
Canal (section is along Pontchartrain Blvd.),
showing portion of geophysical traverses relative
to the buried beach (modified from Reference 13)
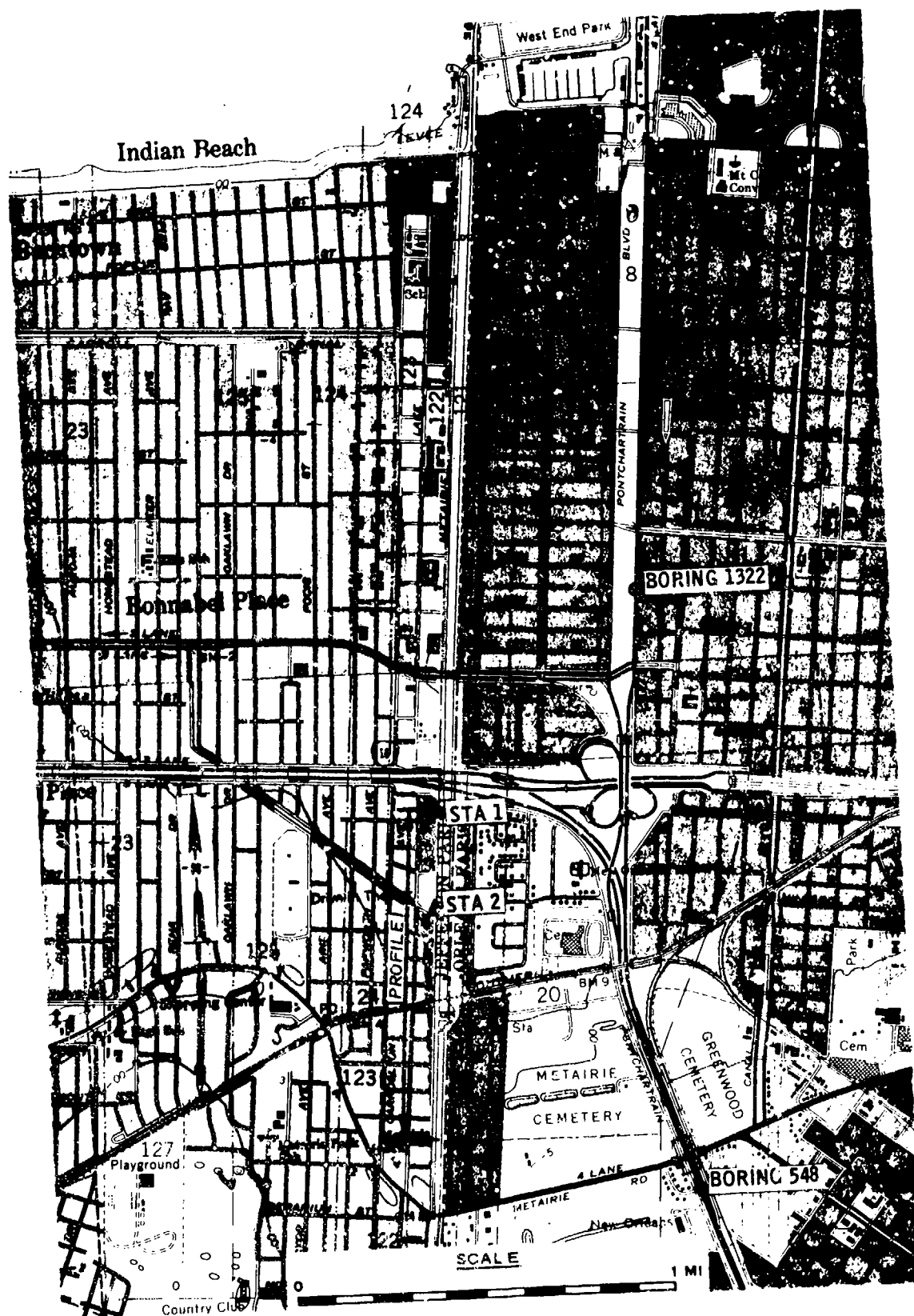
Figure 35. Map of Metairie Outfall Canal site, New Orleans.
Borings delineate position of geologic section of
Figure 34

$V_1 = \dfrac{40}{0.0351} = 1140$ FT/SEC

$V_2 = \dfrac{100-60}{0.0541-0.0438} = 3883$ FT/SEC

$D_1 = \dfrac{V_2 T_{i_2}}{2} \times \dfrac{1}{\sqrt{\left(\dfrac{V_2}{V_1}\right)^2 - 1}} = \dfrac{3983 \times 0.025}{2} \times \dfrac{1}{\sqrt{\left(\dfrac{3883}{1140}\right)^2 - 1}} = 16.8$ FT

$V_2 = 3883$ FT/SEC

$V_1 = 1140$ FT/SEC

DISTANCE, FT

TIME, MSEC

$T_{i_2}$
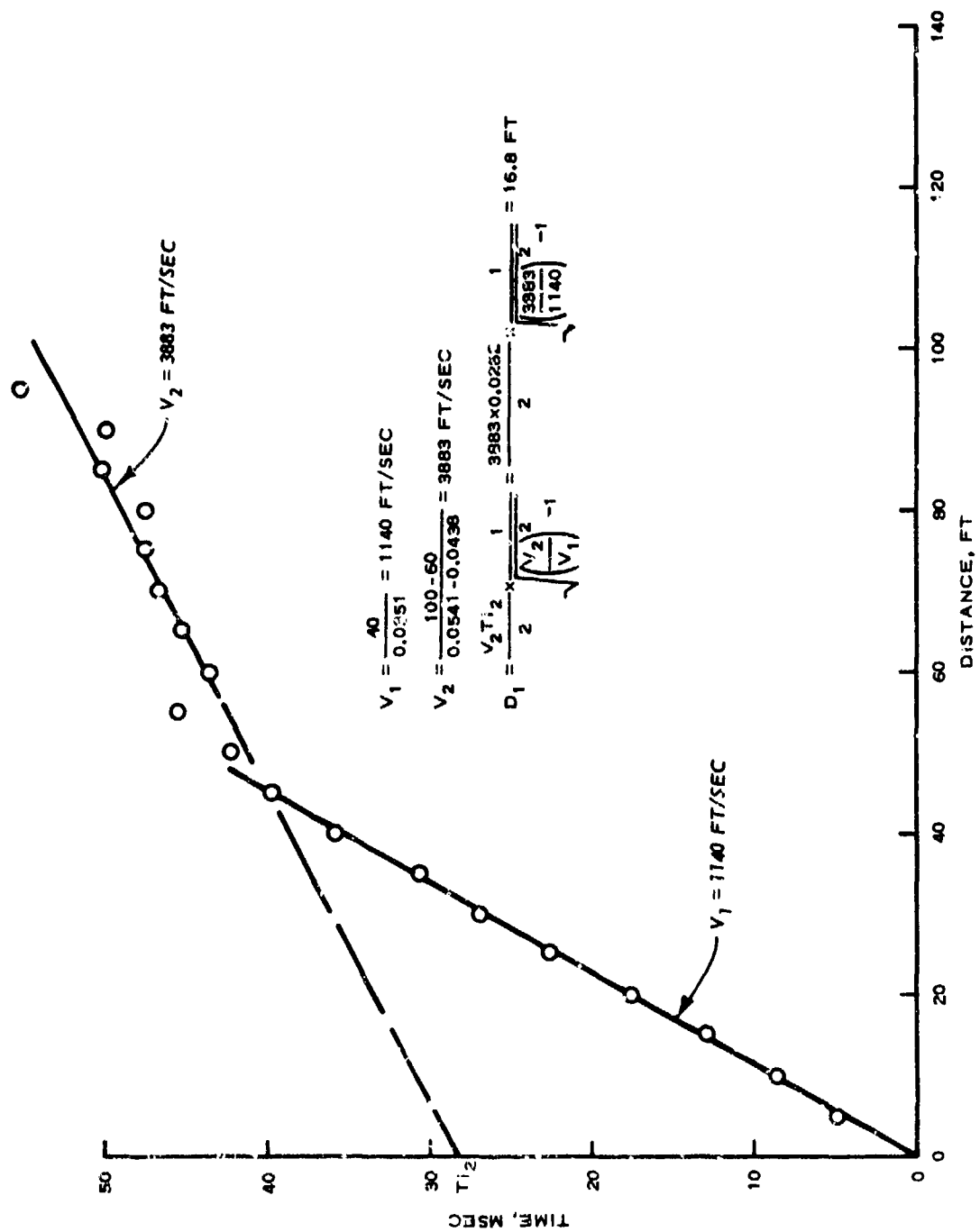
Figure 36. Seismic refraction data, top of levee,
Metairie Outfall Canal site, New Orleans
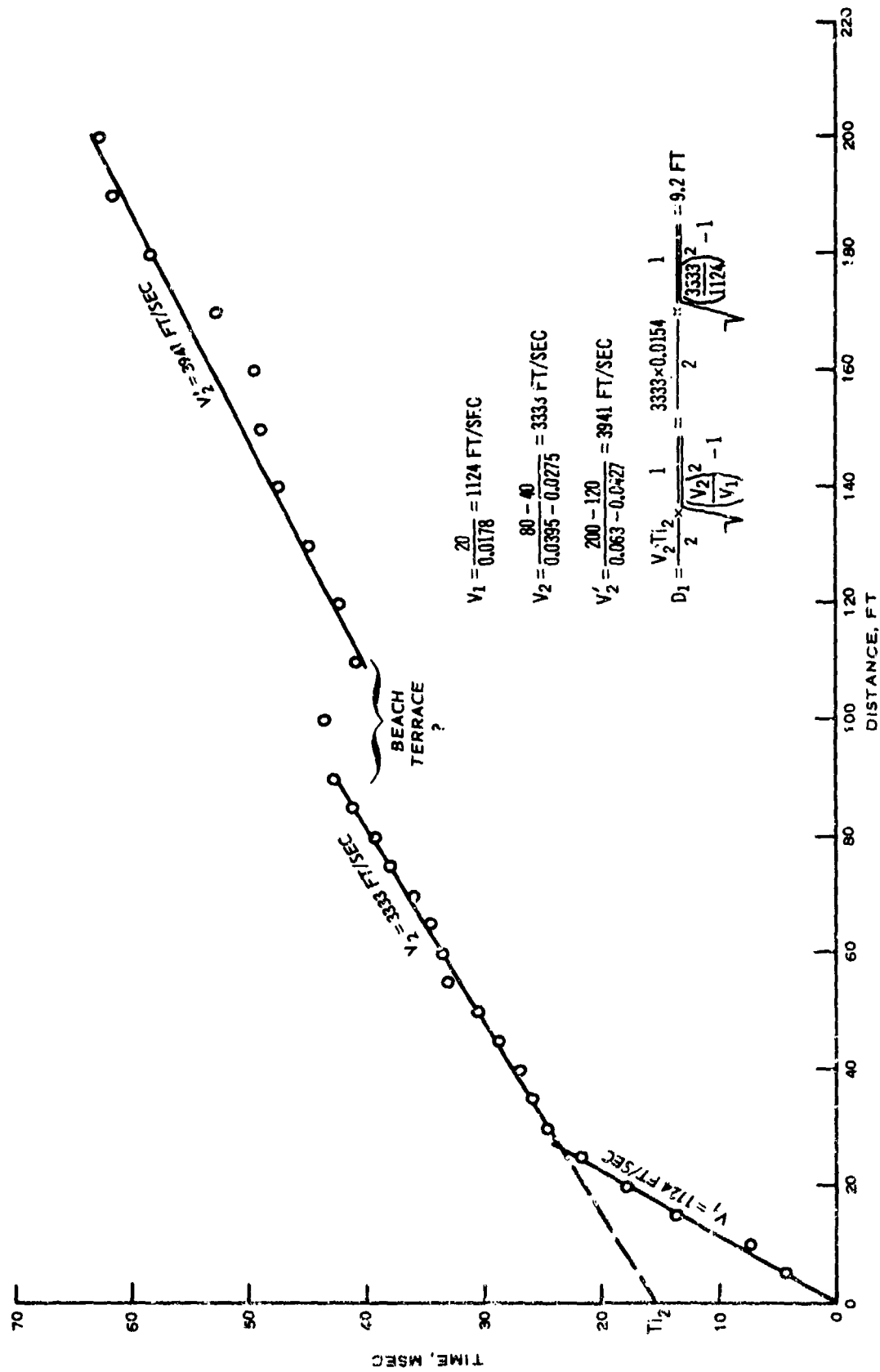
Figure 37. Seismic refraction data, base of levee, Metairie Outfall Canal site, New Orleans
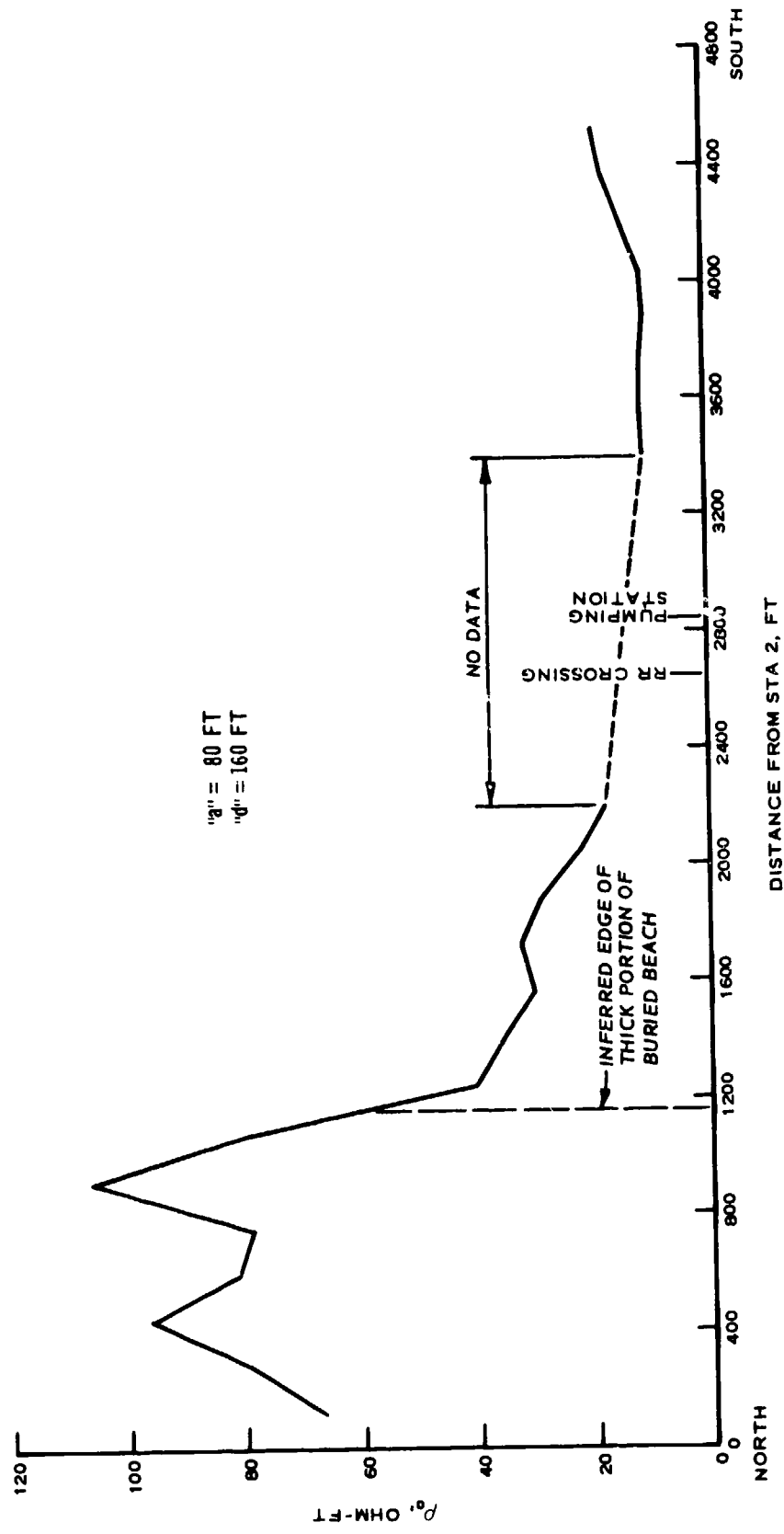
Figure 38. Graph of resistivity profile, Metairie Outfall Canal site, New Orleans
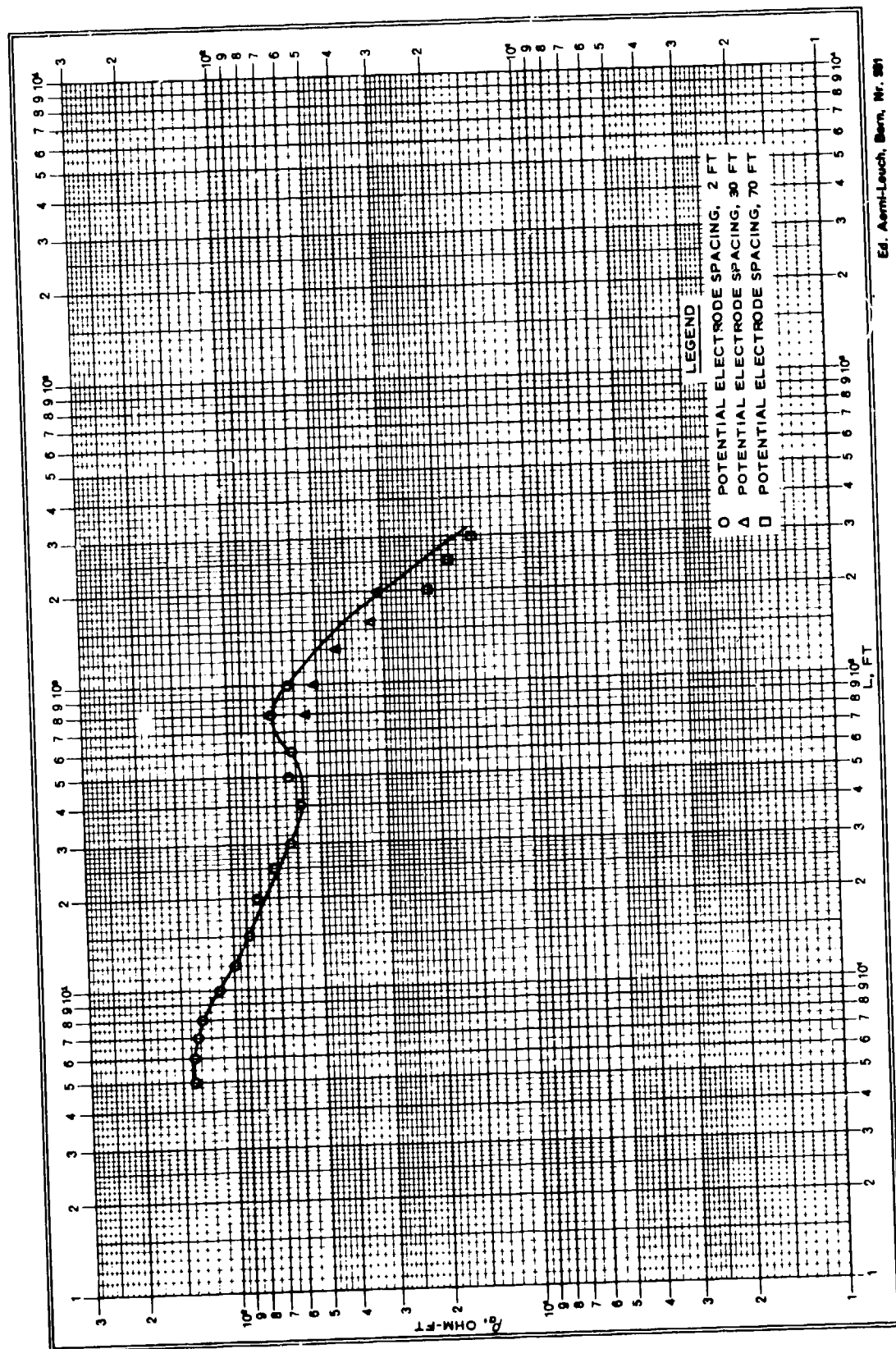
Figure 39. Field curve, resistivity sounding,
Metairie Outfall Canal, New Orleans
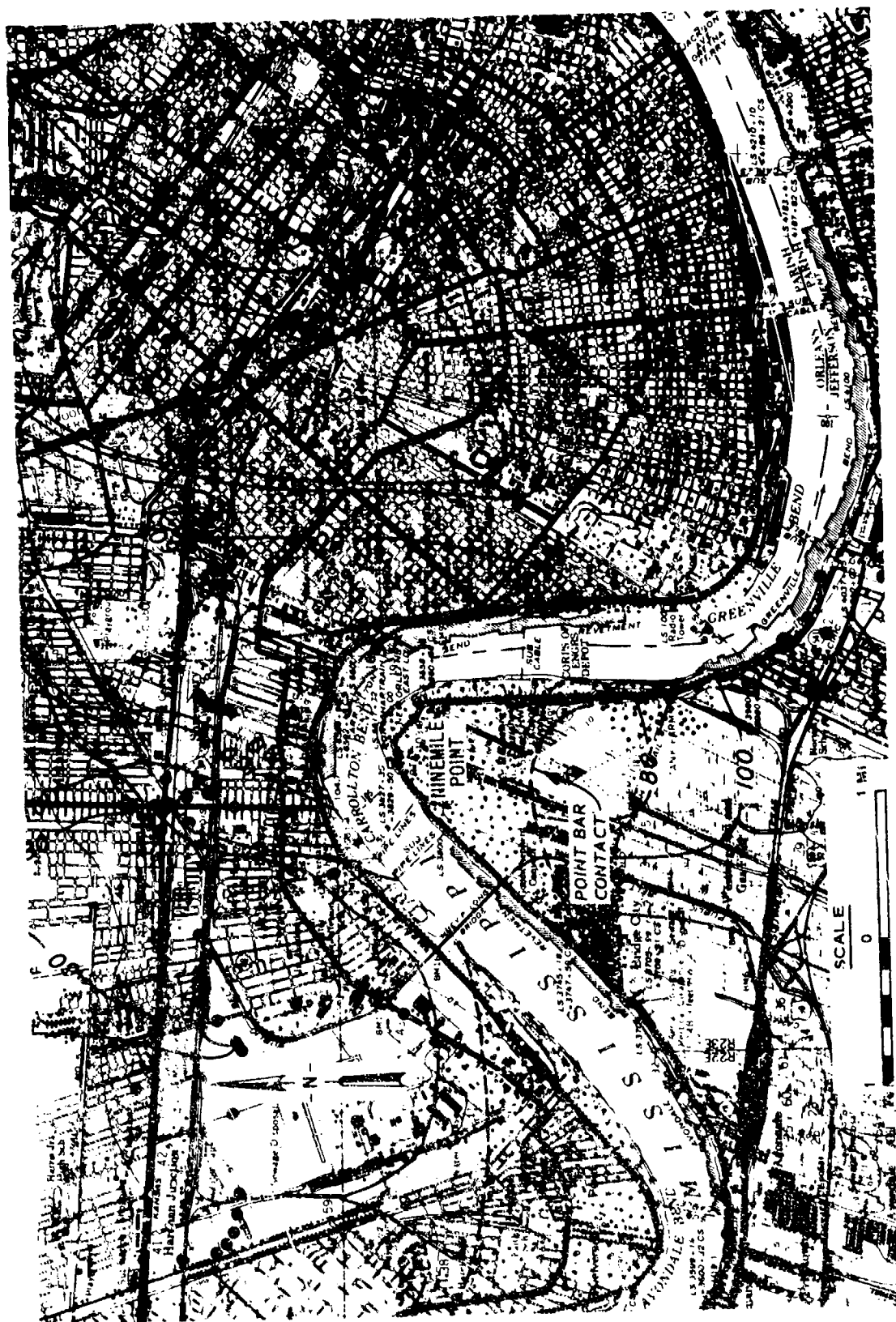
Figure 40. Partial geology of the New Orleans, Nine Mile Point area. Contours are of the top of the Pleistocene (from Reference 14)
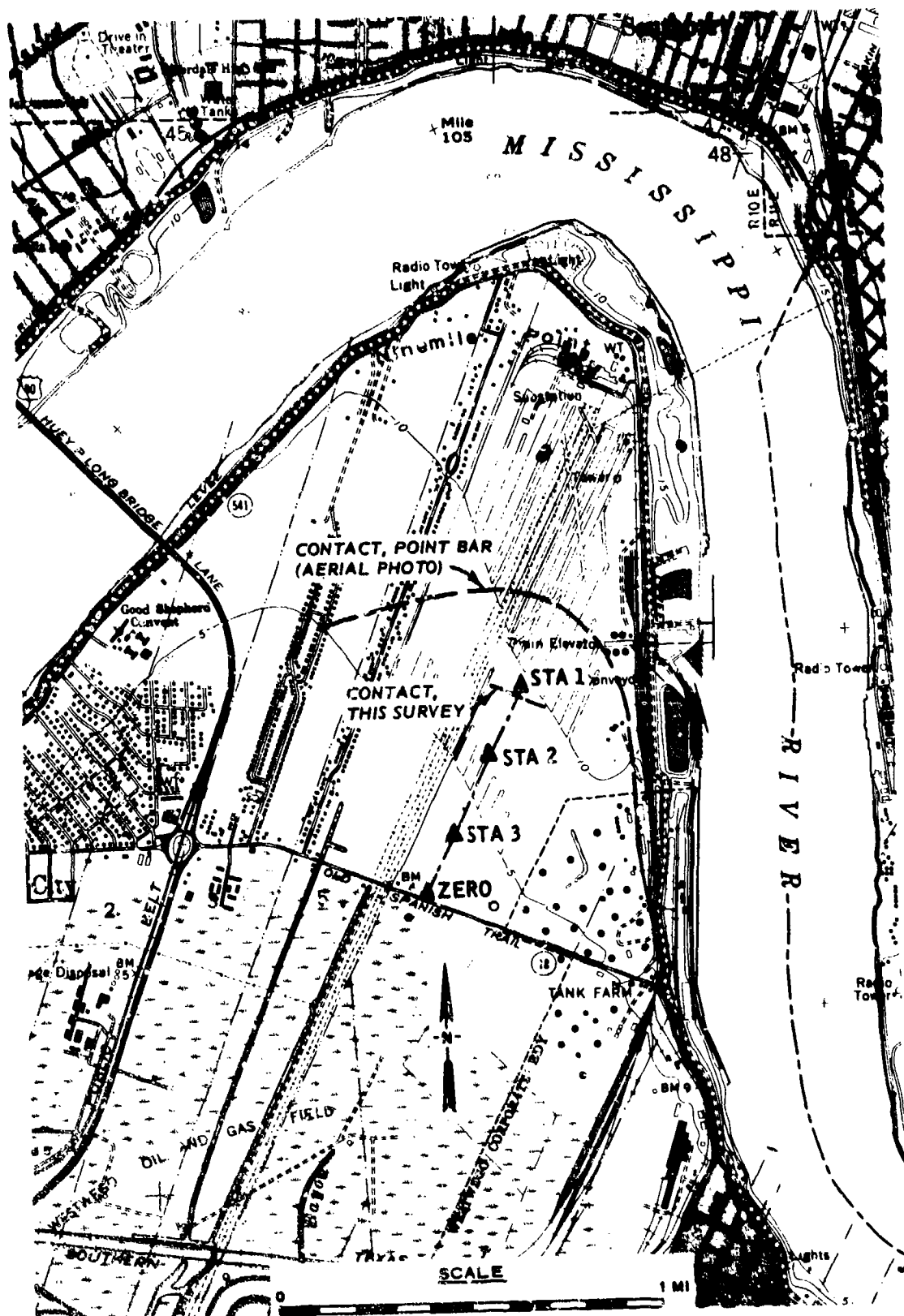
Figure 41. Map of Nine Mile Point site, New Orleans
(from New Orleans West 7-1/2 min quad)
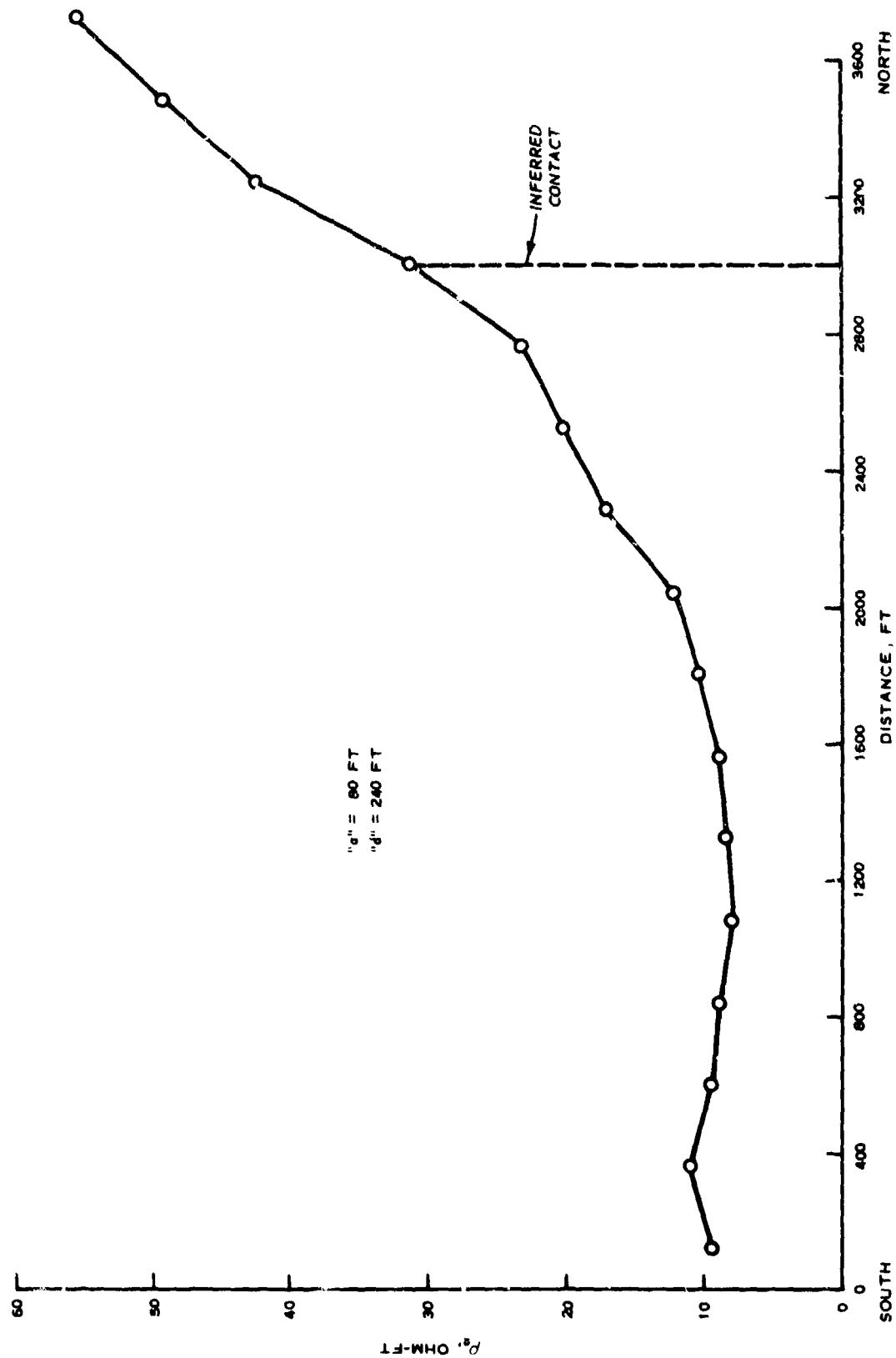
Figure 42. Resistivity profile graph, Nine Mile
Point site, New Orleans
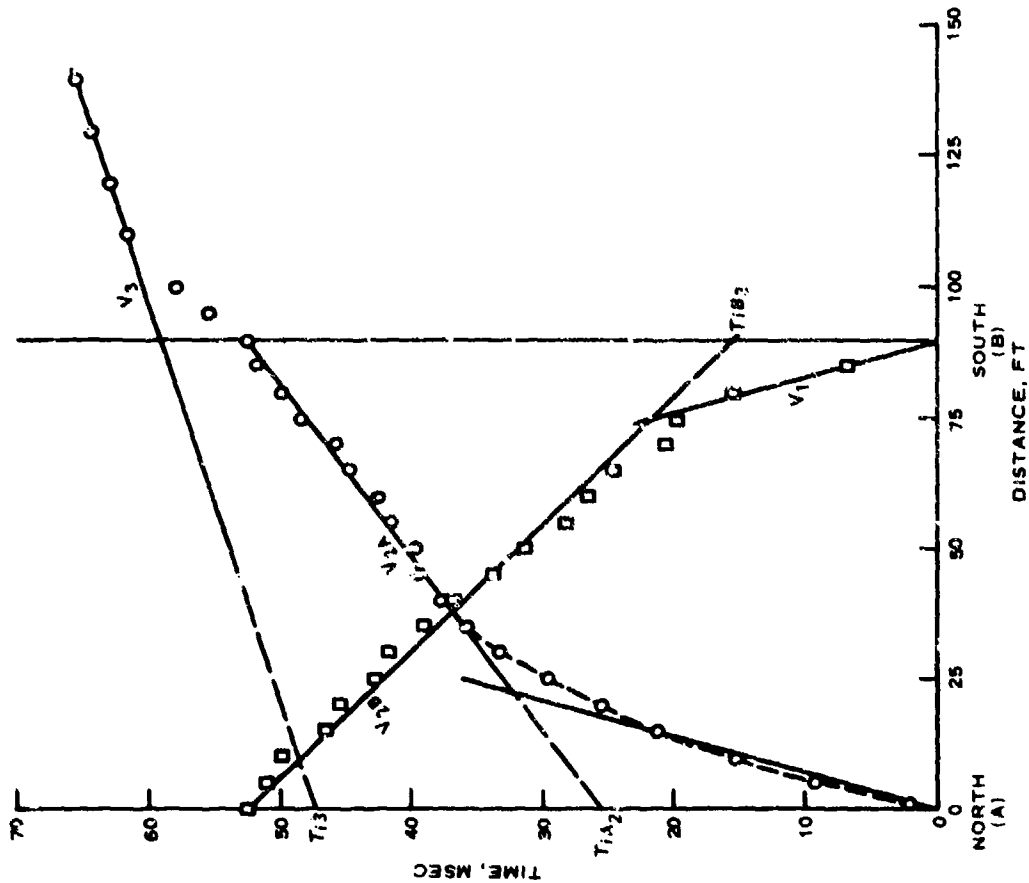
## INTERPRETATION

ASSUME $V_1$ CONSTANT $= \dfrac{21 \text{ FT}}{0.030 \text{ SEC}} = 700$ FT/SEC

$V_{2A} = \dfrac{90}{0.0525 - 0.0253} = 3308$ FT/SEC  $V_{2B} = \dfrac{90}{0.0525 - 0.0156} = 2439$ FT/SEC

$\text{Dip} = \theta = \tfrac{1}{2}\left[\sin^{-1}\dfrac{V_1}{V_{2B}} - \sin^{-1}\dfrac{V_1}{V_{2A}}\right] = \tfrac{1}{2}\left[\sin^{-1}\dfrac{700}{2439} - \sin^{-1}\dfrac{700}{3308}\right] = 2.2^\circ$ NORTH

$V_2 = 2\cos\theta\ \dfrac{V_{2A} \times V_{2B}}{V_{2A} + V_{2B}} = 2(0.999)\dfrac{3308 \times 2439}{3308 + 2439} = 2812$ FT/SEC

DEPTH AT A $= D_A = \dfrac{1}{\cos\theta} \times \dfrac{V_1 T_{iA}}{2} \ \dfrac{1}{\sqrt{1 - \left(\dfrac{V_1}{V_2}\right)^2}} = \dfrac{700 \times 0.0254}{2} \times \dfrac{1}{\sqrt{1 - \left(\dfrac{700}{2808}\right)^2}} = 9.5$ FT

DEPTH AT B $= D_B = \dfrac{1}{\cos\theta} \times \dfrac{V_1 T_{iB}}{2} \ \dfrac{1}{\sqrt{1 - \left(\dfrac{V_1}{V_2}\right)^2}} = \dfrac{700 \times 0.0156}{2} \times \dfrac{1}{\sqrt{1 - \left(\dfrac{700}{2808}\right)^2}} = 5.8$ FT

DEPTH TO THIRD LAYER BASED ON CURVE A $= D_2$

$V_3 = \dfrac{125}{0.0637 - 0.0475} = 7716$ FT/SEC

$D_2 = \dfrac{V_3 T_{i_2}}{2} \times \sqrt{\dfrac{1}{\left(\dfrac{V_3}{V_2}\right)^2 - 1}} - D_1 \dfrac{\sqrt{\left(\dfrac{V_3}{V_2}\right)^2 - 1}}{\sqrt{\left(\dfrac{V_3}{V_2}\right)^2 - 1}}$   WHERE $D_1 = D_A$

$= \dfrac{7716 \times 0.0475}{2} \times \dfrac{1}{\sqrt{\left(\dfrac{7716}{2808}\right)^2 - 1}} - 9.5 \left[\dfrac{\sqrt{\left(\dfrac{7716}{700}\right)^2 - 1}}{\sqrt{\left(\dfrac{7716}{2808}\right)^2 - 1}}\right] = 40.4$ FT

Figure 43. Seismic refraction data, sta 1,
Nine Mile Point site, New Orleans
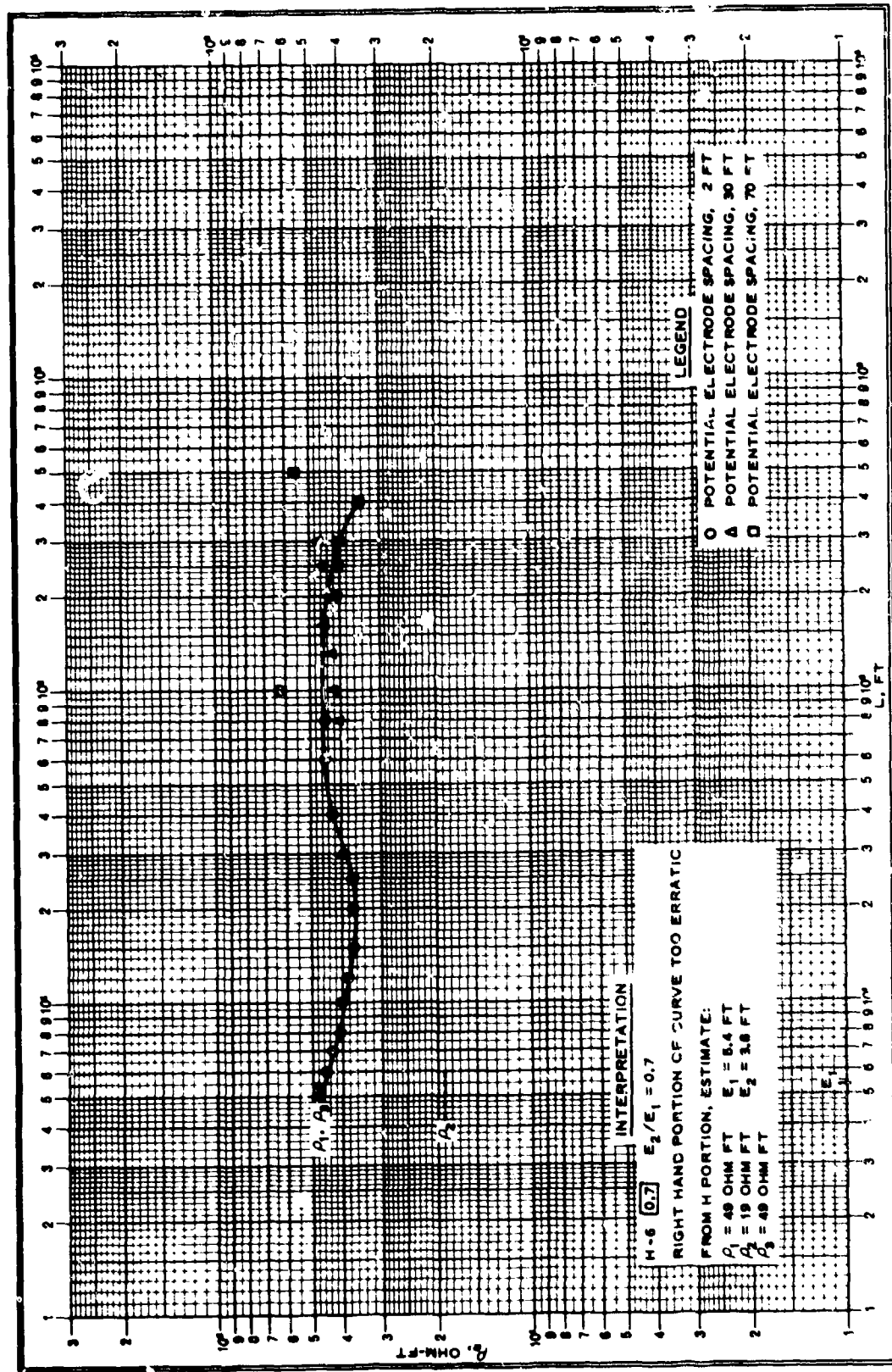
Figure 44. Field curve, resistivity sounding,
str 1, Nine Mile Point site, New Orleans
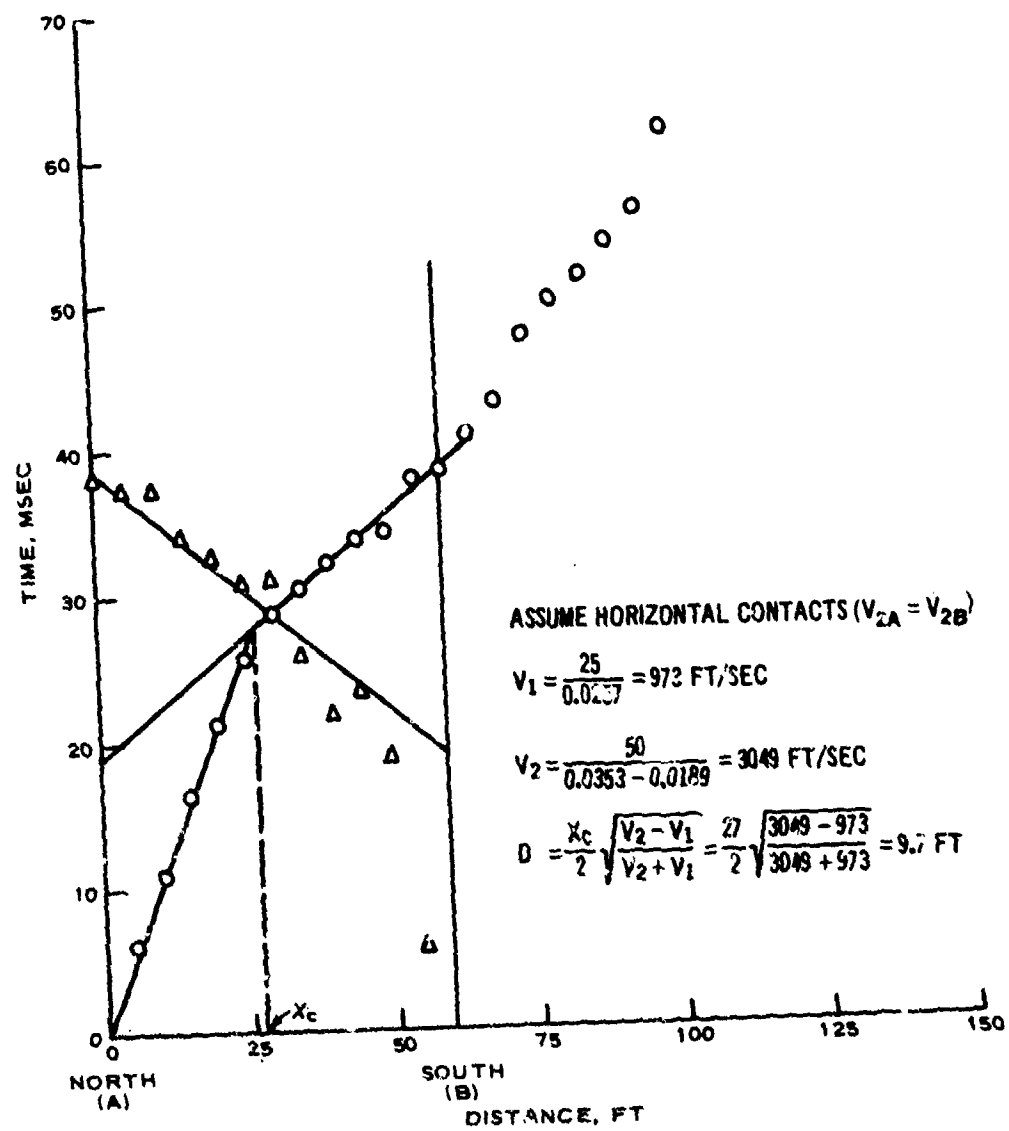
Figure 45. Seismic refraction data, sta 2, Nine Mile Point site, New Orleans
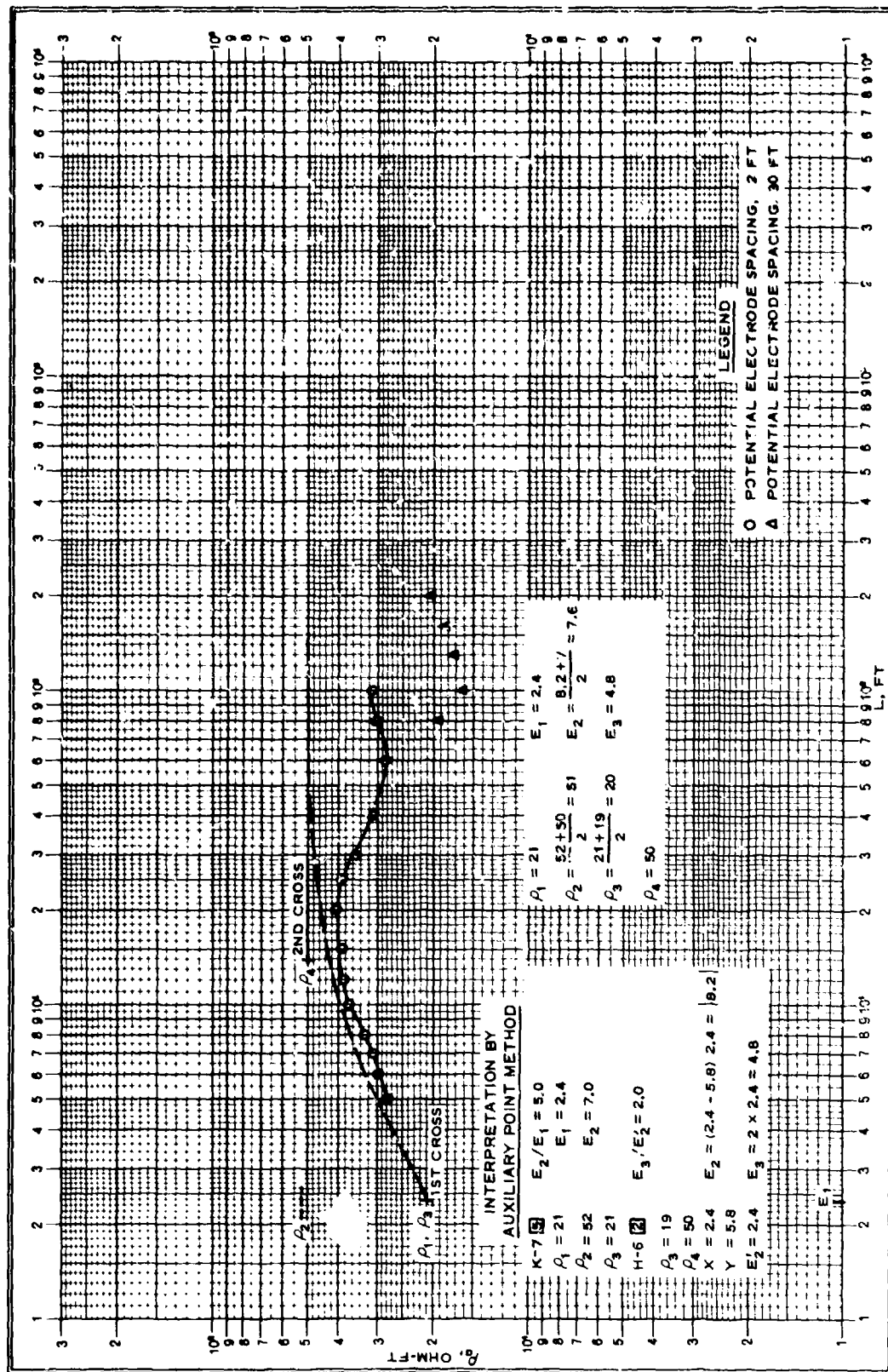
Figure 46.  Field curve, resistivity sounding, sta 2,
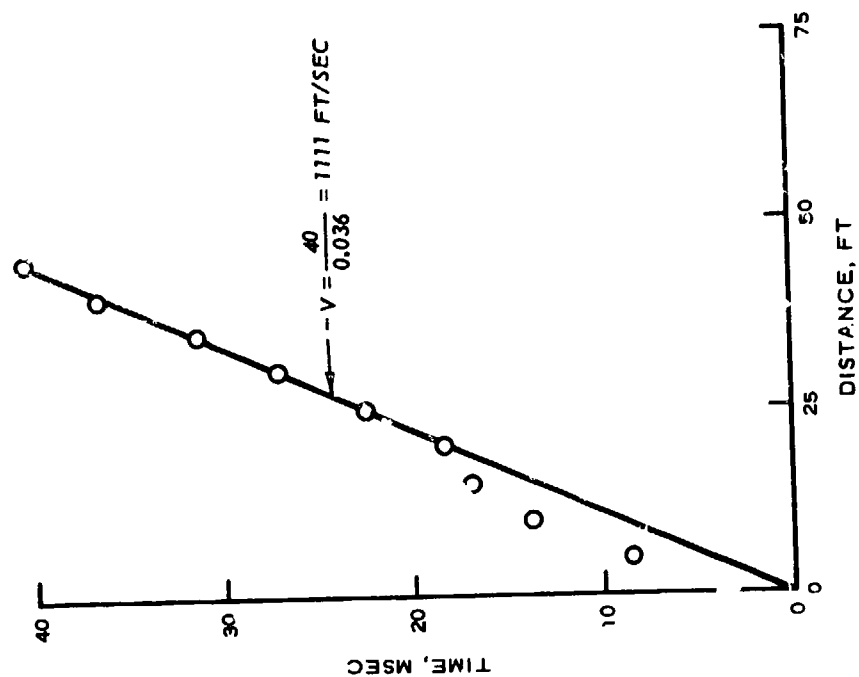Nine Mile Point site, New Orleans

Figure 47. Seismic refraction data, sta. 3,
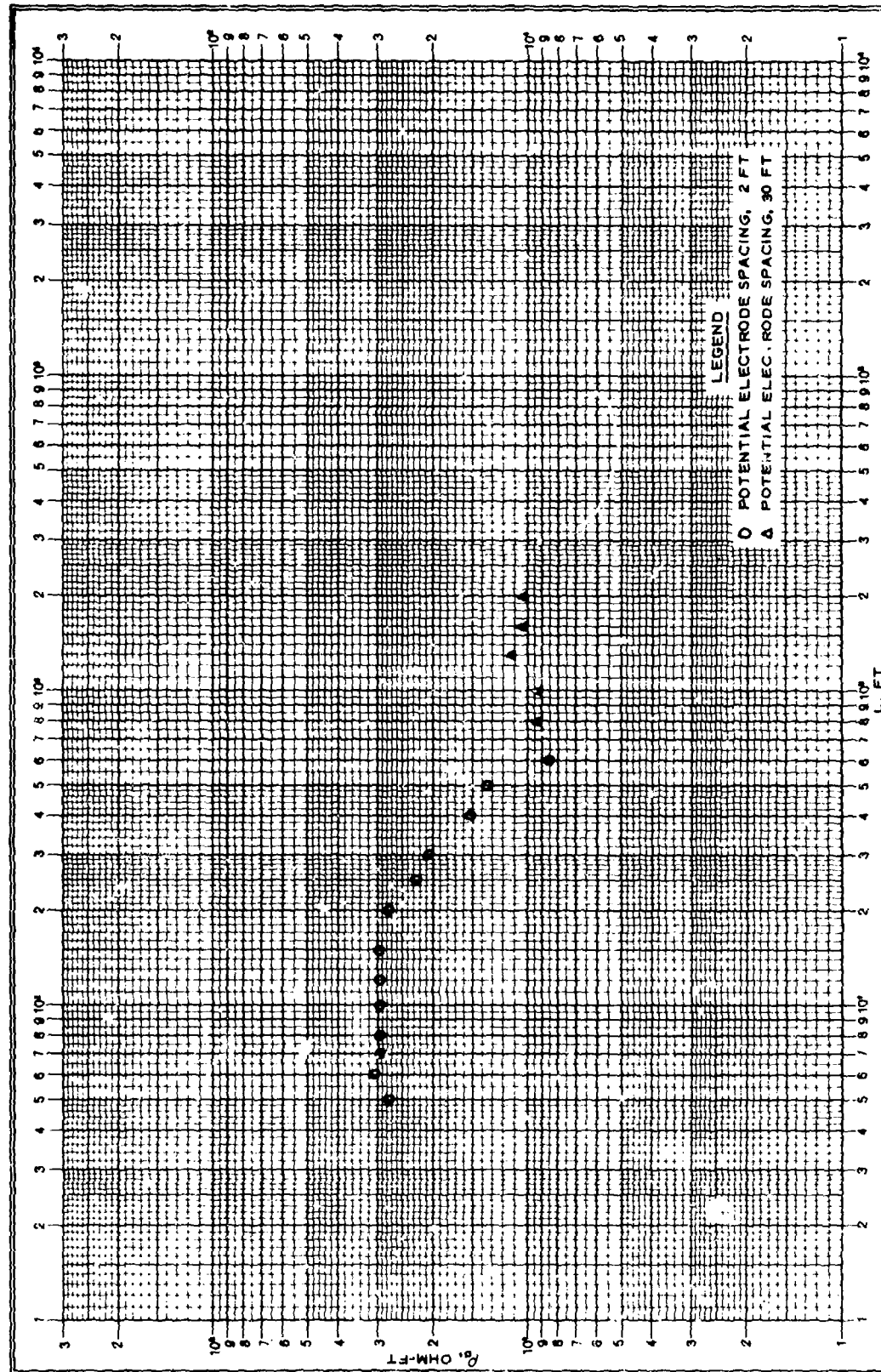Nine Mile Point site, New Orleans

Figure 48. Field curve, resistivity sounding, sta 3, Nine Mile Point site, New Orleans